DOE/SF/18852--T61

Cassini RTG Program CDRL Transmittal

TO: U.S. Department of Energy 6633 Canoga Avenue Canoga Park, California 91303 Attention: K. Vijaiyan Project Manager	Cassini RTG Program Contract No: DE-AC03-91SF18852	In Reply Refer to: **CON #1502** Date: **24 March 1996**
	CDRL Number: **Reporting Requirement 4.F (Document No. RR16)**	
	Title: **Monthly Technical Progress Report (29 January 1996 through 25 February 1996)**	
	Approval Requirements: Approval ☐ None ☒	
	Contract Period: **11 January 1991 through 30 April 1998**	

DISTRIBUTION:

Symbol	*Copies*
A	5
B	1
C	1
D	1
E	2
H	2
J	20
K	1

INTRODUCTION

The technical progress achieved during the period 29 January though 25 February 1996 on Contract DE-AC03-91SF18852 Radioisotope Thermoelectric Generators and Ancillary Activities is described herein.

This report is organized by program task structure.

- 1.X Spacecraft Integration and Liaison
- 2.X Engineering Support
- 3.X Safety
- 4.X Qualified Unicouple Production
- 5.X ETG Fabrication, Assembly, and Test
- 6.X Ground Support Equipment (GSE)
- 7.X RTG Shipping and Launch Support
- 8.X Designs, Reviews, and Mission Applications
- 9.X Project Management, Quality Assurance, Reliability, Contract Changes, CAGO Acquisition (Operating Funds), and CAGO Maintenance and Repair
- H.X CAGO Acquisition (Capital Funds)

Note: Task H.X scope is included in SOW ¶ Task 9.5.
Task H. was created to manage CAGO acquired with capital equipment funding.

Approved: R. J. Hemler
R. J. Hemler, Manager
Space Power Programs

Internal Distribution:
Technical Report List

From: Lockheed Martin Missiles & Space
Room 10B50 Building B
720 Vandenberg Road
King of Prussia, PA 19406

Signature: Joseph M. Waks

Joseph M. Waks
Contracts Manager

Monthly Technical Report
Progress by Major Task

TASK 1 SPACECRAFT INTEGRATION AND LIAISON

The capacitance test was performed on the E-7 converter and the test data forwarded to JPL for evaluation. Attention will shift to planning the measurement of end dome temperatures on the F-2 generator during thermal vacuum testing at Mound later this spring.

TASK 2 ENGINEERING SUPPORT

Specifications/Drawings

ECNs for the ETG/RTG activities were prepared and processed through CCB approval. The System Specification GPHS-RTG for Cassini (23009149) and the Environmental Criteria and Test Requirements GPHS-RTG for Cassini Specification (23009150) have been approved by DOE and are in the process of being issued.

RTG Fuel Form, Fueling, and Test Support/Liaison

Work continued, as necessary, on the evaluation and disposition of fuel processing related non-conformance reports from LANL. In a related task, after reviewing available information and in consultation with other program participants, concurrence was given to revising the LANL fuel specifications. The revisions dealt primarily with impurity requirements, and updated specifications will be issued in the near future.

TASK 3 SAFETY ANALYSIS TASK

The safety analysis task is comprised of four major activities: 1) Launch Accident Analysis; 2) Reentry Analysis; 3) Consequence and Risk Analysis and 4) the Safety Test Program. An overview of the significant issues related to this task for this period, followed by details in each of the four major activities, is provided in the following subsections.

A listing of the INSRP meetings held through February 1996 is provided in Table 3-1. One INSRP review was held in this reporting period with the Reentry Subpanel (RESP) at Aerospace Corporation in El Segundo, CA. The status of nominal trajectory VVEJGA

Table 3-1. Safety Analysis Task – Completed INSRP Reviews

Date	*Review*
14 February 1995	INSRP PSAR Review
20 April 1995	PSSP Review of LASEP-T Status
27 April 1995	RESP Review of Reentry CFD and Thermal Analysis
3 May 1995	MET Review of SPARRC Status
16 May 1995	BEES Review of SPARRC Status
8 June 1995	Working Meeting with INSRP on Launch Accident Analysis Treatment of Variability and Uncertainty
10 August 1995	RESP Review of Reentry CFD and Thermal Analysis
23 August 1995	LASP Review of PSAR Comments and Databook Items
24 August 1995	INSRP Review of Launch Accident Analysis Treatment of Variability and Uncertainty
19 September 1995	Review Meeting with INSRP MET Chairperson
28 September 1995	Working Meeting with INSRP on Reentry Analysis Treatment of Variability and Uncertainty
25-27 October 1995	INSRP PSSP Review of LASEP-T and RESP Review of Reentry
6-8 November 1995	MET and BEES Review of SPARRC Status
29-30 November 1995	INSRP Safety Analysis and Status Review
17-19 January 1996	INSRP Review of LASEP-T and Out-of-Orbit Preliminary Analysis Results
13-14 February 1996	RESP Review of VVEJGA and Out-of-Orbit Preliminary Reentry Analysis Results

reentry calculations was reviewed along with out-of-orbit recession calculations. Planned treatment of variability and uncertainty within the VVEJGA and out-of-orbit reentry risk analyses was presented to the RESP as well.

Launch Accident Analysis

The model documentation for Version 1.0 of the LASEP-T code was completed. Documents were distributed to DOE and INSRP describing LASEP-T subroutines employed in Version 1.0. Preliminary source terms from LASEP-T Version 1.0 were provided to INSRP during the mid-January review.

Changes to the LASEP-T code were completed in this reporting period to reflect new hydrocode data, incorporate corrections/improvements to the fragment impact and distortion to release models, and to provide better clad traceability algorithms to help track and further verify the LASEP-T results. These refinements were needed to reduce conservatism in the LASEP-T code and to provide more detailed output for additional statistical analyses to be performed. In addition, a post processor was written to collect statistics on individual conditions that resulted in a release. Following verification of these changes, LASEP-T Version 2.0 will be issued to be used for analyses to be presented in the Draft FSAR.

Work on adapting Sandia National Lab's (SNL's) ERAD code has begun. The PUFF subroutine from SNL's ERAD code will handle the plume rise for releases in liquid propellant fireballs. Implementing PUFF has resulted in additional changes to LASEP-T. The vaporization and agglomeration is still handled in the LASEP-T code but the altitude passed to SPARRC is the altitude of release. The SPARRC code will determine the buoyancy rise based on the amount of propellant that is available from the fireball. This propellant weight, along with a reaction efficiency term, is passed as part of the release record and is a function of the type of fireball (core, space vehicle, etc.) and location (air or ground) per Titan IV Databook specifications.

Selected LASEP-T subroutines were passed to Lockheed Martin reentry personnel to be used to simulate ground impact releases as a result of inadvertent out-of-orbit or VVEJGA reentry. These subroutines were modified to be applied outside of the LASEP-T Monte Carlo driver code. Using the LASEP-T models in the reentry analysis ensures consistency in the application of clad distortion and fuel release models as utilized for launch accident simulations.

Weekly telecons have been held with Lockheed Martin (Valley Forge), NASA-Lewis, Lockheed Martin (Denver), JPL, and DOE to discuss topics ranging from the Titan IV Databook to the development of full stack intact impact environments. These telecons focus the resources on key issues related to the FSAR and FSAR addenda.

Sandia National Labs delivered the first operational module of the plutonia vaporization and agglomeration model. This module calculates liquid propellant fireball temperature, rise velocity and size based on reactant mixes provided by NASA-JPL/Foils Engineering hydrocode analysis. Additional modules addressing plutonium transport and heterogeneous agglomeration affects are scheduled for delivery in late March.

Reentry Analysis

Steep Trajectory Results: During the previous reporting period CFD analyses on the steep ($\gamma = 90°$) trajectory had advanced to the fifth (out of ten) trajectory point, with globally converged RACER (flowfield)/LORAN-C (radiation) solutions obtained. Subsequent SINRAP transient heating runs revealed that the specified wall temperature upper bound for the fifth trajectory point was too low. The front face temperature was therefore increased from 7610°R to 7910°R. Table 3-2 lists the freestream environment and imposed surface temperatures (updated for point 5) for the steep trajectory.

Table 3-2. Steep Trajectory Cases

Trajectory Point	Time (sec)	Velocity (kft/sec)	Altitude (kft)	T_{front} (°R)	T_{side} (°R)
1	0.0	63.834	258.000	2360	2330
				2410	2380
				2460	2430
2	0.3	63.762	238.864	3460	2460
				3960	2760
				4460	3060
3	0.6	63.586	219.764	5960	2560
				6460	2960
				6960	3360
4	1.1	62.752	188.149	6460	2960
				6960	3460
				7460	3960
5	1.6	60.214	157.306	6960	3460
				7460	3960
				7910	4110

The 300°R increase in wall temperature proved to have a dramatic effect on the surface energy balance terms. Initially, the RACER code required small time steps to obtain a stable solution. This problem was resolved by invoking more frequent radiation field (LORAN-C) updates in the global iteration process. In this case, the incident surface radiation is a strong function of the ablation rate (because of carbon absorption) and both must be closely coupled as the solution evolves.

An earlier version of Figures 3-1 through 3-9 appeared in the January Monthly Technical Progress Report. Similar results were also presented at the 13-14 February INSRP/RESP meeting. These figures have now been updated to incorporate results for the new high wall temperature solution at 1.6 seconds (trajectory point 5).

The prescribed front face wall temperatures for the steep trajectory are compared to the converged SINRAP transient heating solution for the shallow trajectory in Figure 3-1. Note that since the duration of the heat pulse for the steep trajectory is expected to be about one-tenth of the time incurred along the shallow trajectory, the figure includes a steep trajectory time scale that is one-tenth that of the shallow trajectory.

The components of the heat flux are compared in Figure 3-2. The "convective" component includes gas conduction plus diffusion due to species gradients. At 1.6 seconds along the steep trajectory, both the radiative and convective components decrease as the wall temperature is increased. The total heat flux to the surface for the steep and shallow trajectories is shown in Figure 3-3. An increase of 950°R in the wall temperature (comparing

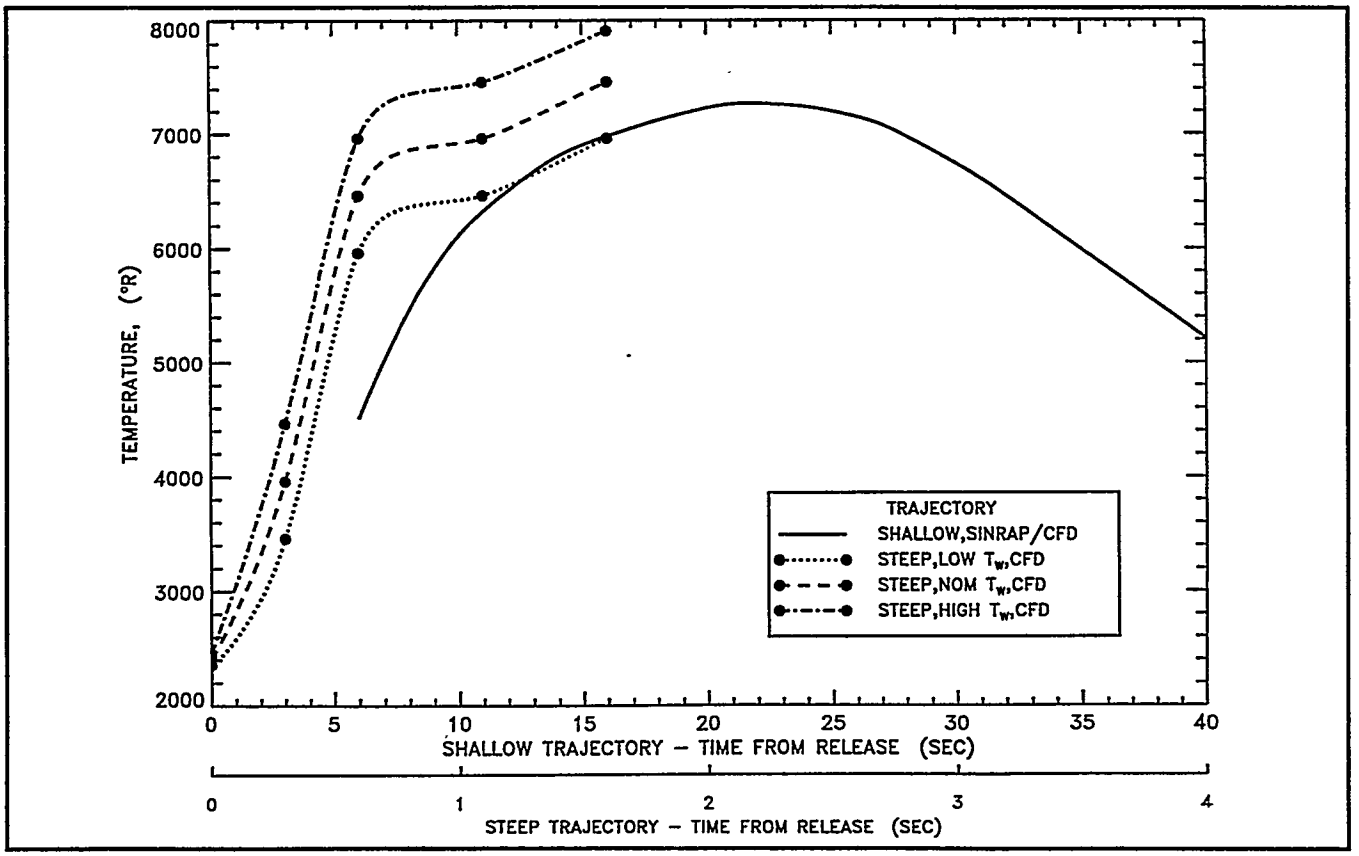

Figure 3-1. Steep Trajectory Computational Matrix. Comparison with Converged SINRAP Temperature History for the Shallow Trajectory

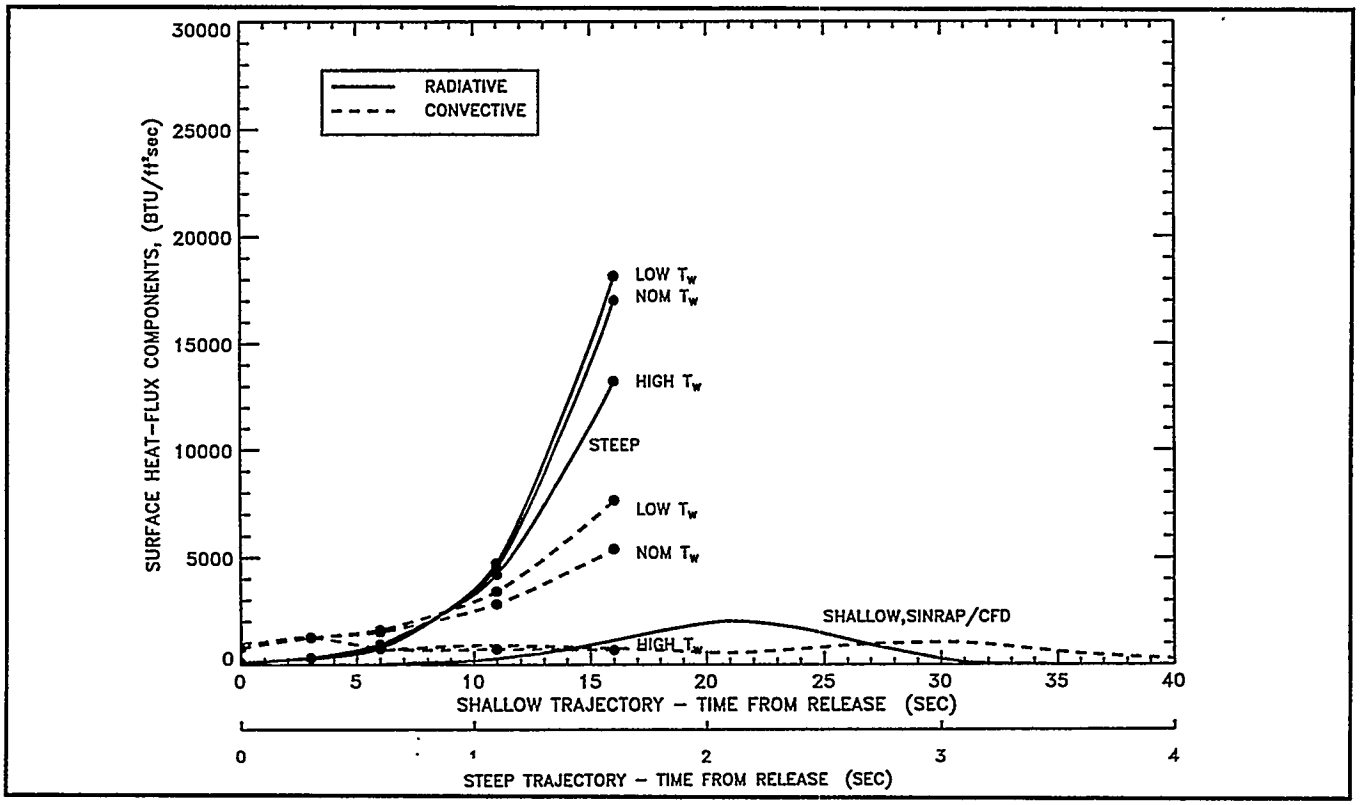

Figure 3-2. Comparison of the Heat Flux Components along the Steep Trajectory with the SINRAP Shallow Trajectory Solution

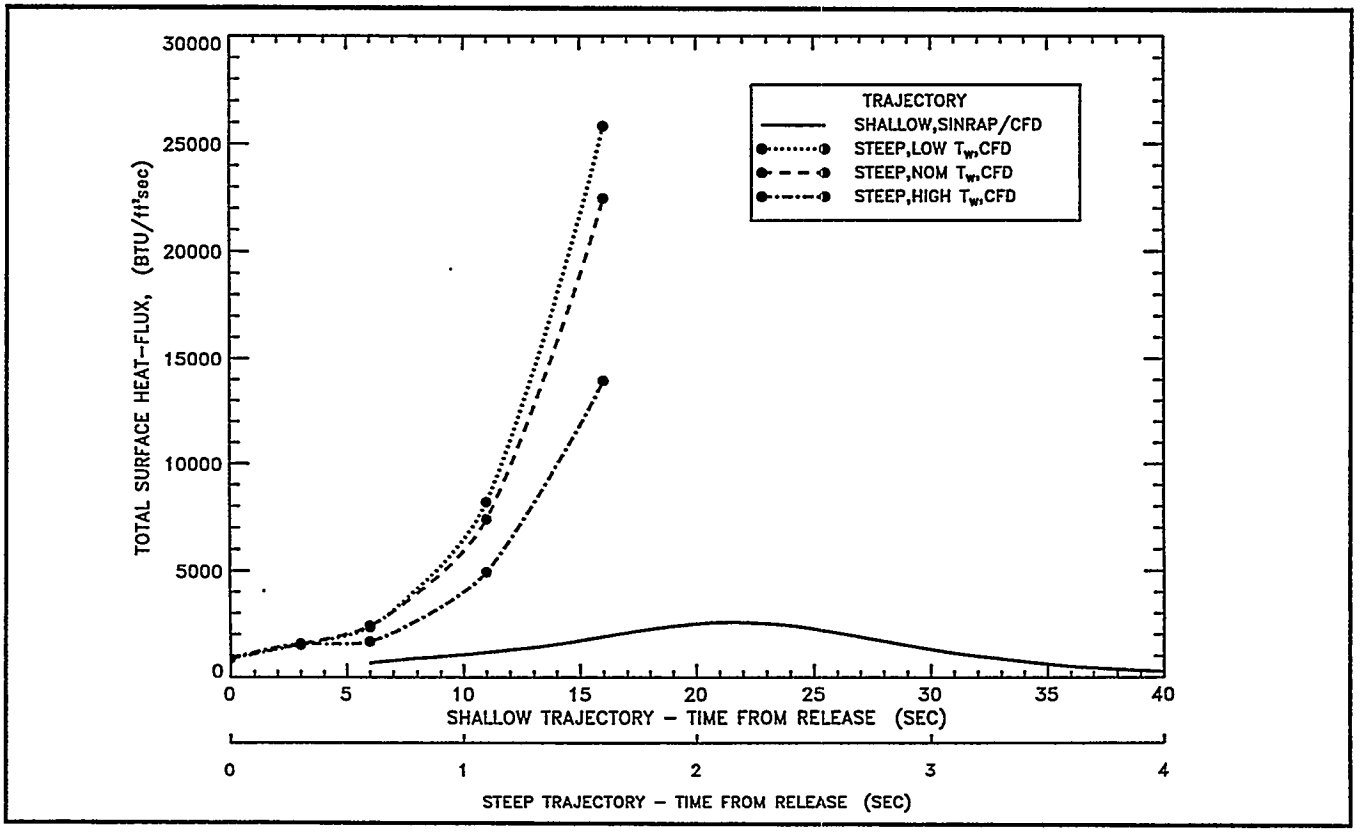

Figure 3-3. Comparison of the Total Heat Flux along the Steep Trajectory with the SINRAP Shallow Trajectory Solution

the "low" to the "high" wall temperature case) for the fifth steep trajectory point causes a drop of 12,000 BTU/(ft^2-sec). The ablation rate results, shown in Figure 3-4, clearly show an exponential increase as the wall temperature is increased. At the highest wall temperature at 1.6 seconds, the ablation rate is about 0.56 lb_m/(ft^2 - sec).

Detailed flow and chemistry results along the stagnation streamline are compared in Figures 3-5 through 3-9. The shallow peak heating case (M_∞ = 50.7, altitude = 58.6 Km, T_w = 7260°R) is compared with the high wall temperature, case 5, on the steep trajectory (M_∞ = 55.9, altitude = 48.0 Km, T_w = 7910°R). The stagnation streamline pressure distributions are shown in Figure 3-5. The shock layer pressure is about four atmospheres for the steep but less than one atmosphere for the shallow. The shock layer temperature for the steep case, shown in Figure 3-6, reaches nearly 22,000°K (39,600°R). The peak shock layer temperature for the shallow case is less at about 18,000°K (32,400°R). The stagnation streamline density, shown in Figure 3-7, is over four times higher for the steep case. The

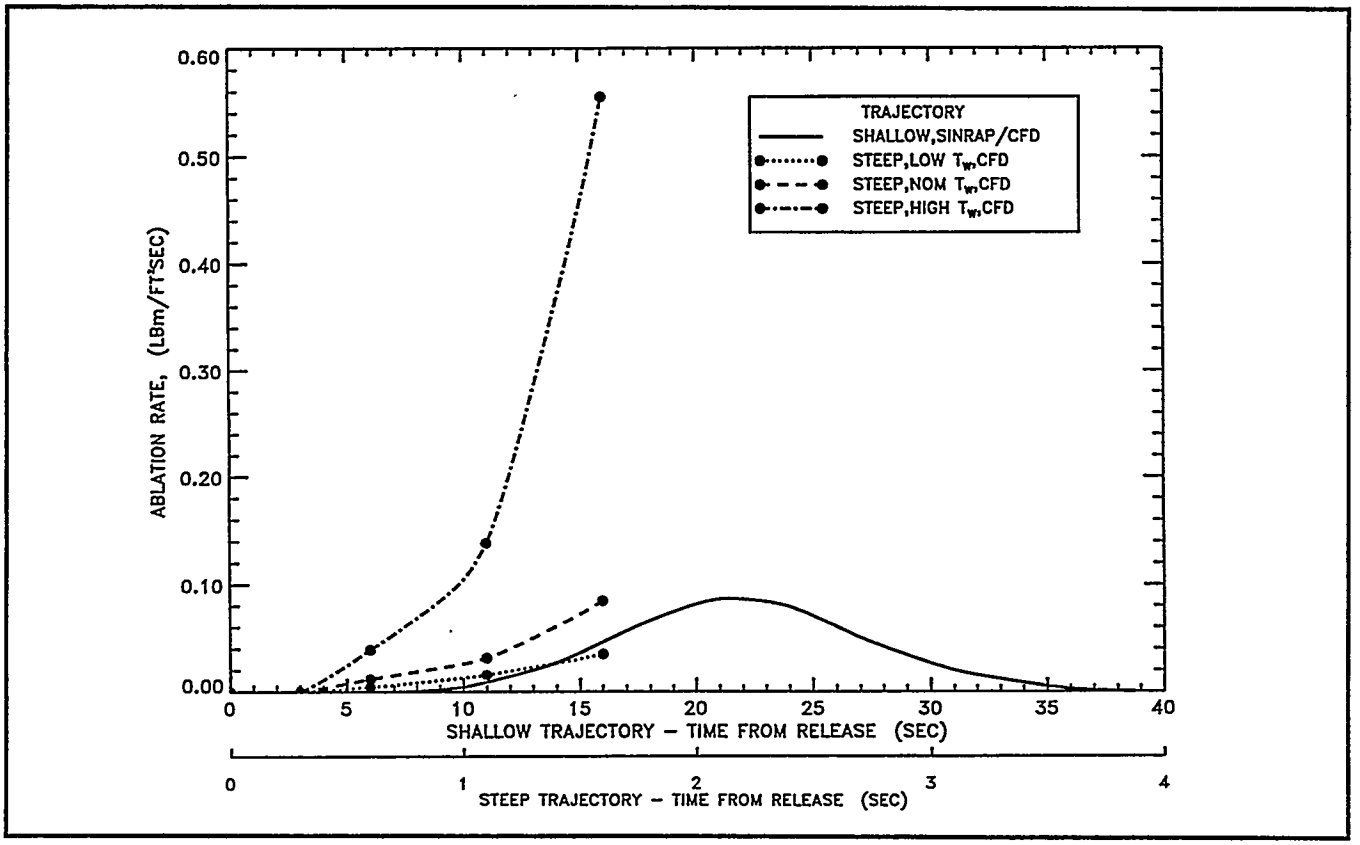

Figure 3-4. Comparison of the Ablation Rate along the Steep Trajectory with the SINRAP Shallow Trajectory Solution

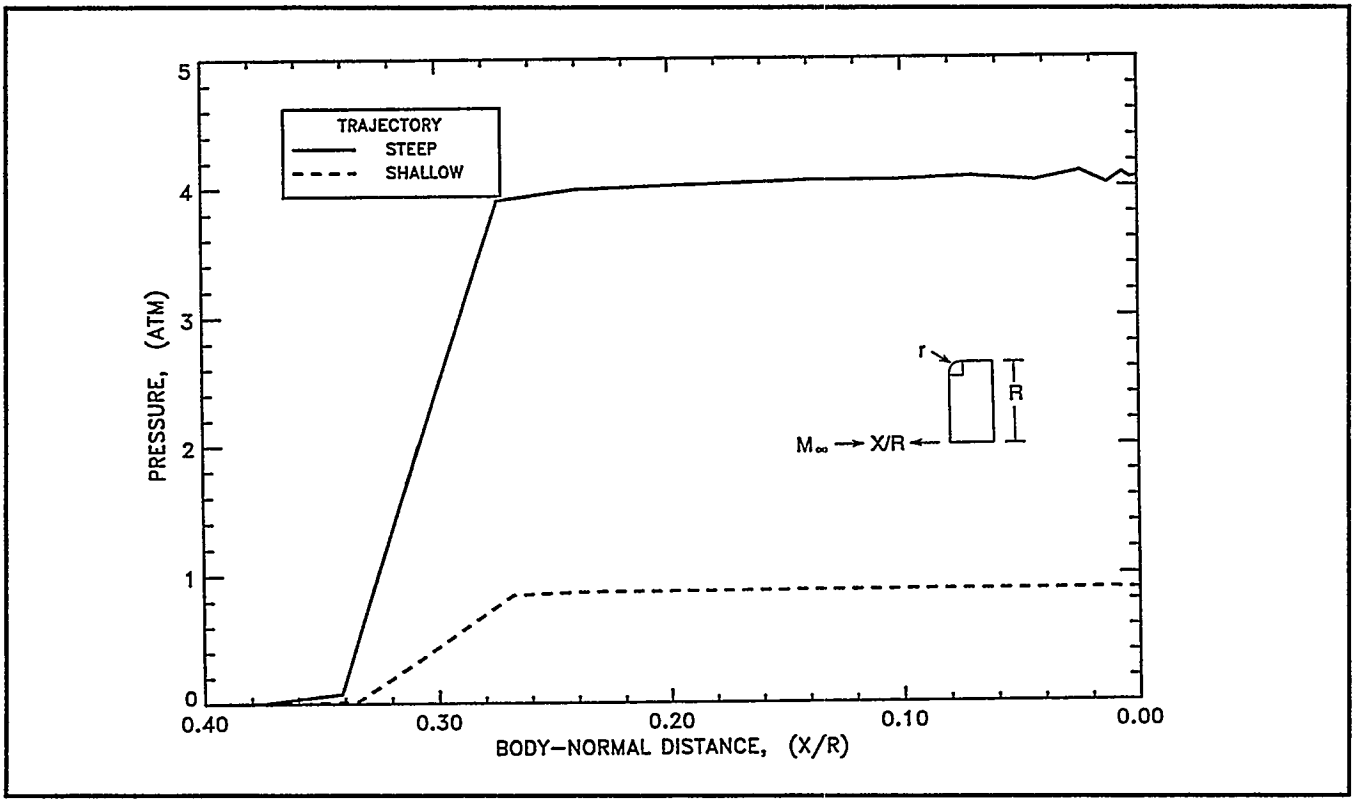

Figure 3-5. Stagnation Streamline Pressure Distribution. Comparison of Steep Case 5 (High T_w) with Shallow Peak Heating

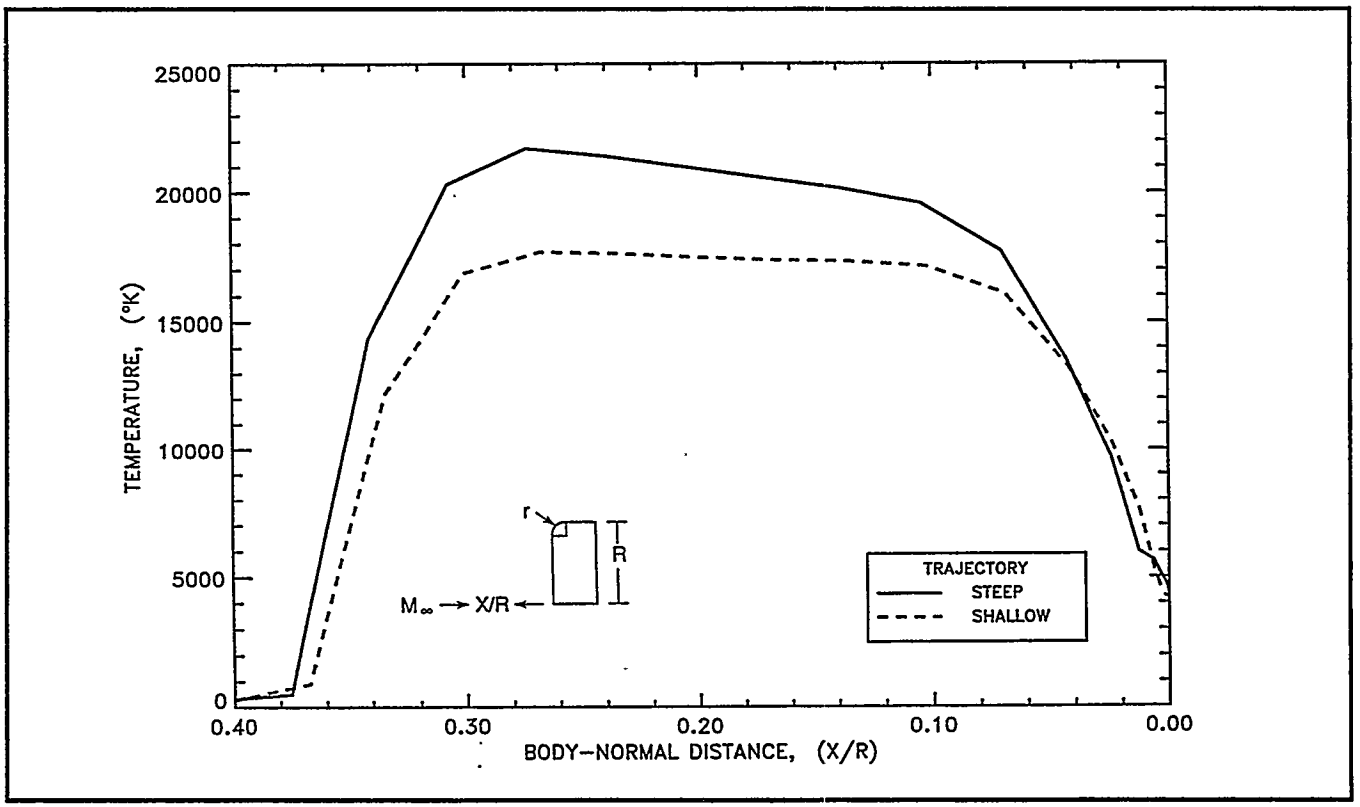

Figure 3-6. Stagnation Streamline Temperature Distribution. Comparison of Steep Case 5 (High T_w) with Shallow Peak Heating

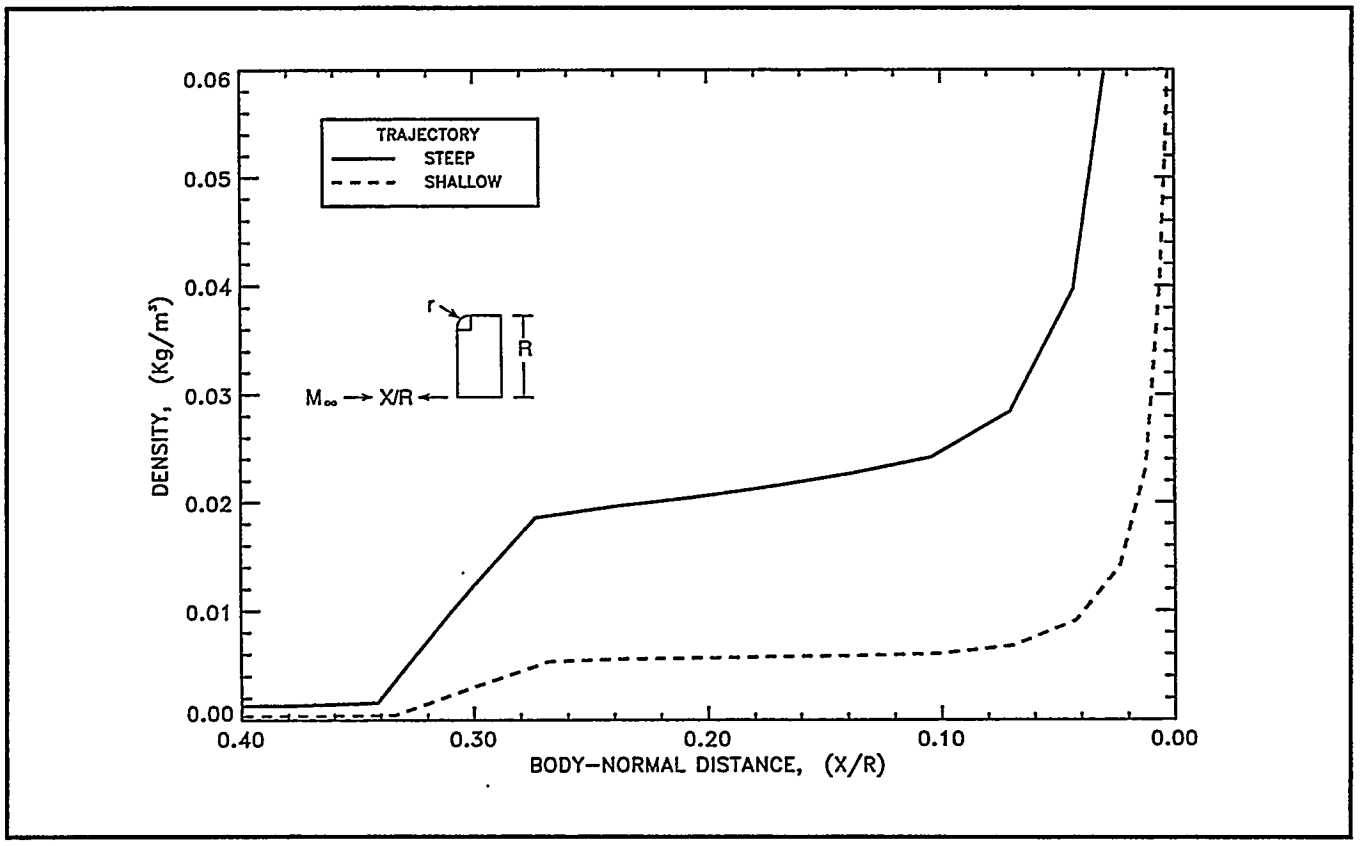

Figure 3-7. Stagnation Streamline Density Distribution. Comparison of Steep Case 5 (High T_w) with Shallow Peak Heating

stagnation streamline carbon species distributions (with mass fractions greater than 0.001) are shown for the shallow and steep cases in Figures 3-8 and 3-9, respectively. The higher ablation rate of the steep case overcomes its higher flowfield density so that the carbon species penetrate a comparable distance into the shock layer for both cases.

Work in Progress: Global iterations are in progress for the sixth and seventh points along the steep trajectory. Experience gained with the fifth trajectory point, namely, the need to more closely couple the radiation and flowfield updates, should alleviate computational difficulties.

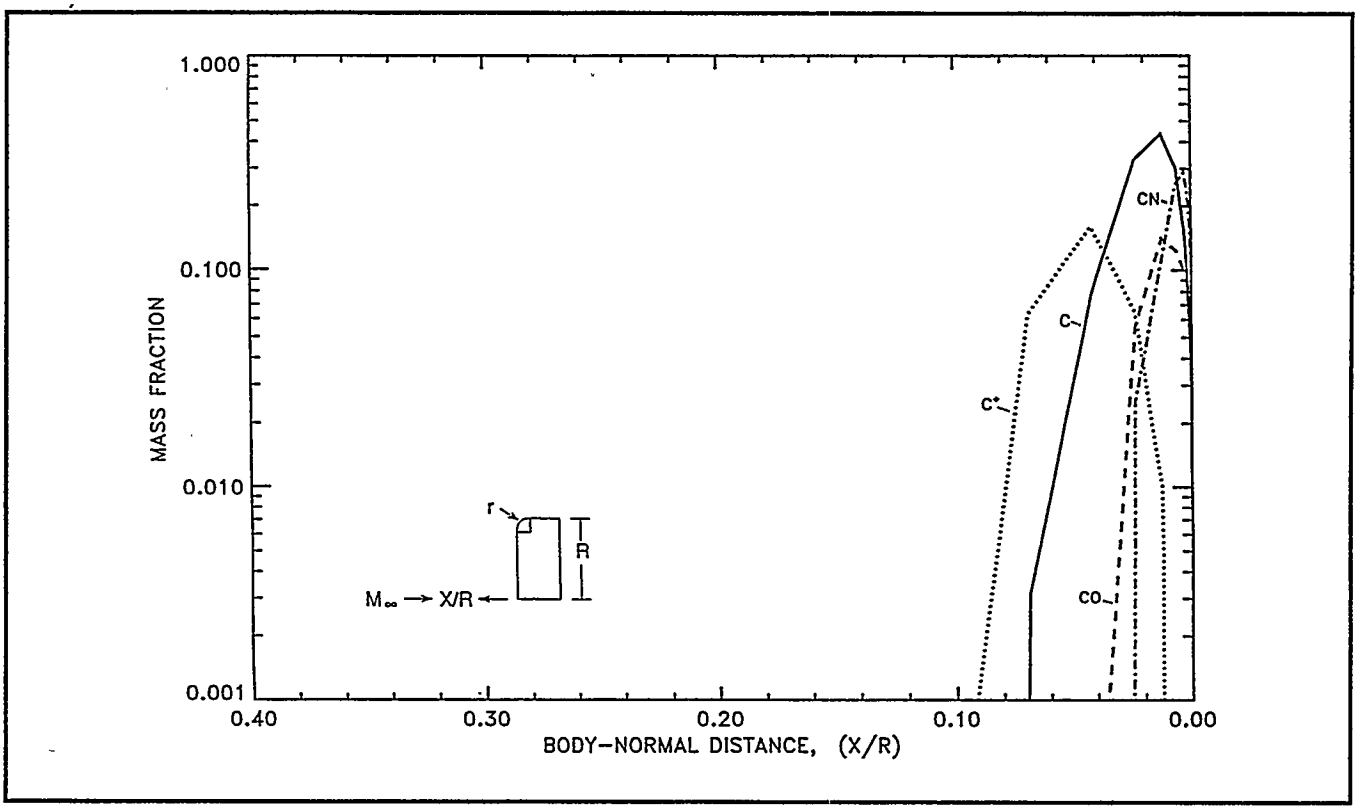

Figure 3-8. Carbon Species along the Stagnation Streamline. Shallow Peak Heating Solution

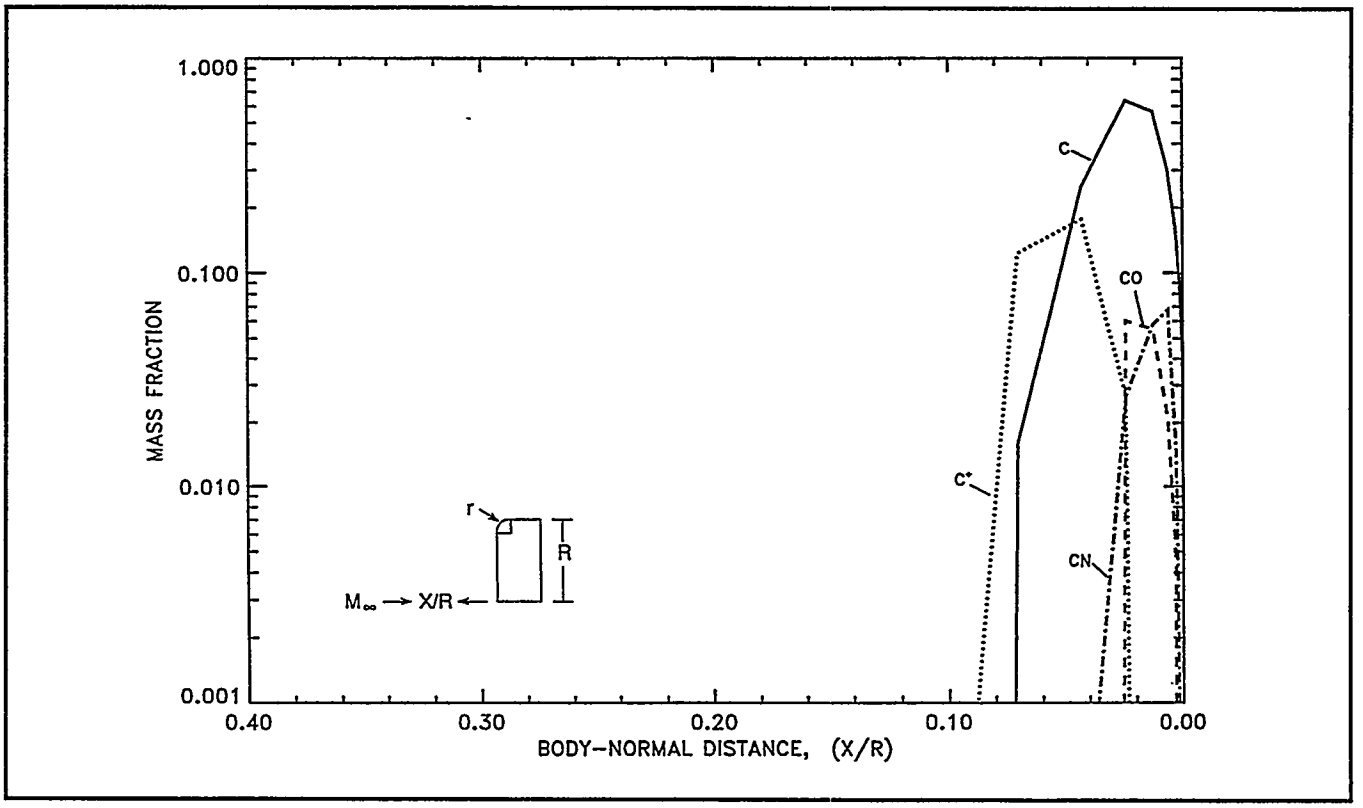

Figure 3-9. Carbon Species along the Stagnation Streamline. Steep Case 5 (High T_w) Solution

Reentry Thermal Analysis

The major effort during the early part of the month involved final preparation for and presentations at the INSRP RESP meeting held 13-14 February at the Aerospace Corporation in El Segundo, CA. Additional accomplishments are as follows:

Steep Trajectory: For the steep trajectory, the CFD results for the first five trajectory points have been incorporated into SINRAP. The CFD results, which were shown last month are shown again in Table 3-3 for completeness. For trajectory point #5 the highest wall temperature for CFD convergence to date is 7150°F. The SINRAP analysis at 1.6 seconds required extrapolation of the surface energy parameters to a much higher temperature. For this reason, the SINRAP calculated temperature at 1.6 seconds turned out to be unreasonably high. The CFD results for 1.6 seconds will also have some influence on the temperature between 0.6 and 1.6 seconds since the time span covers the second set of three altitudes used for interpolation. With this as background, Figure 3-10 shows the stagnation node temperature vs. altitude for the first 1.1 seconds. Also shown are the imposed surface temperatures for the CFD runs as a function of altitude. The relatively low heating rates at the high altitudes caused the calculated temperature to be below the expected range based on past analyses. However, the calculated temperatures for the first three points were used to select the correct range of imposed temperature for the fourth point at 1.1 seconds and altitude of 188,149 ft. The calculated recession at 1.1 seconds is only 0.0016 inches. Therefore, any inaccuracies as a result of the extrapolation at high altitudes will have a negligible effect on the final recession. Peak heating for the steep case is expected to occur at approximately 2.3 seconds at an altitude of 118,505 feet.

Intermediate Angle: Effort was initiated to determine the angle for intermediate trajectory analyses. The intent is to choose an angle which will define the limit of aeroshell survivability from a thermal/structural standpoint. To determine the relative effect of the angle range on recession and temperature, thermal analysis was initiated for entry angles of 50° and 30°. The analysis will be performed with the modules in the random tumbling mode using SINRAP Rev. B. The results for 30° and 50° will be compared to previous random tumbling results for 7° and 90°. The outcome of this study, coupled with the structural analysis, will be used to determine the intermediate angle for CFD and SINRAP Rev. C analyses.

Table 3-3. CFD Results at Stagnation Point - Steep Trajectory

Trajectory Point #	Time (Sec)	Altitude (Ft)	Surface Temperature (°F)	$Q_{RAD}\left(\frac{Btu}{Ft^2 \cdot S}\right)$	$Q_{CONV}\left(\frac{Btu}{Ft^2 \cdot S}\right)$	$\dot{m}\left(\frac{lbm}{Ft^2 \cdot S}\right)$	$\sum_{i=1}^{3} m_{i\omega} h_{i\omega}\left(\frac{Btu}{Ft^2 \cdot S}\right)$
1	0	258000	1900	94	774	.0	0
			1950	94	774	.0	0
			2000	93	774	.0	0
2	0.3	238864	3000	275	1245	.0	0
			3500	301	1252	.0	0
			4000	302	1257	.0	0
3	0.6	219764	4500	838	1739	.000016	0
			5500	806	1611	.0041	76
			6500	941	738	.0391	667
4	1.1	188149	6000	4752	3438	.0155	264
			6500	4554	2843	.0314	537
			7000	4225	715	.1384	2370
5	1.6	157306	6500	19617	8027	.0362	617
			7000	17412	5444	.0864	1490
			7150	17411	4559	.1217	2099

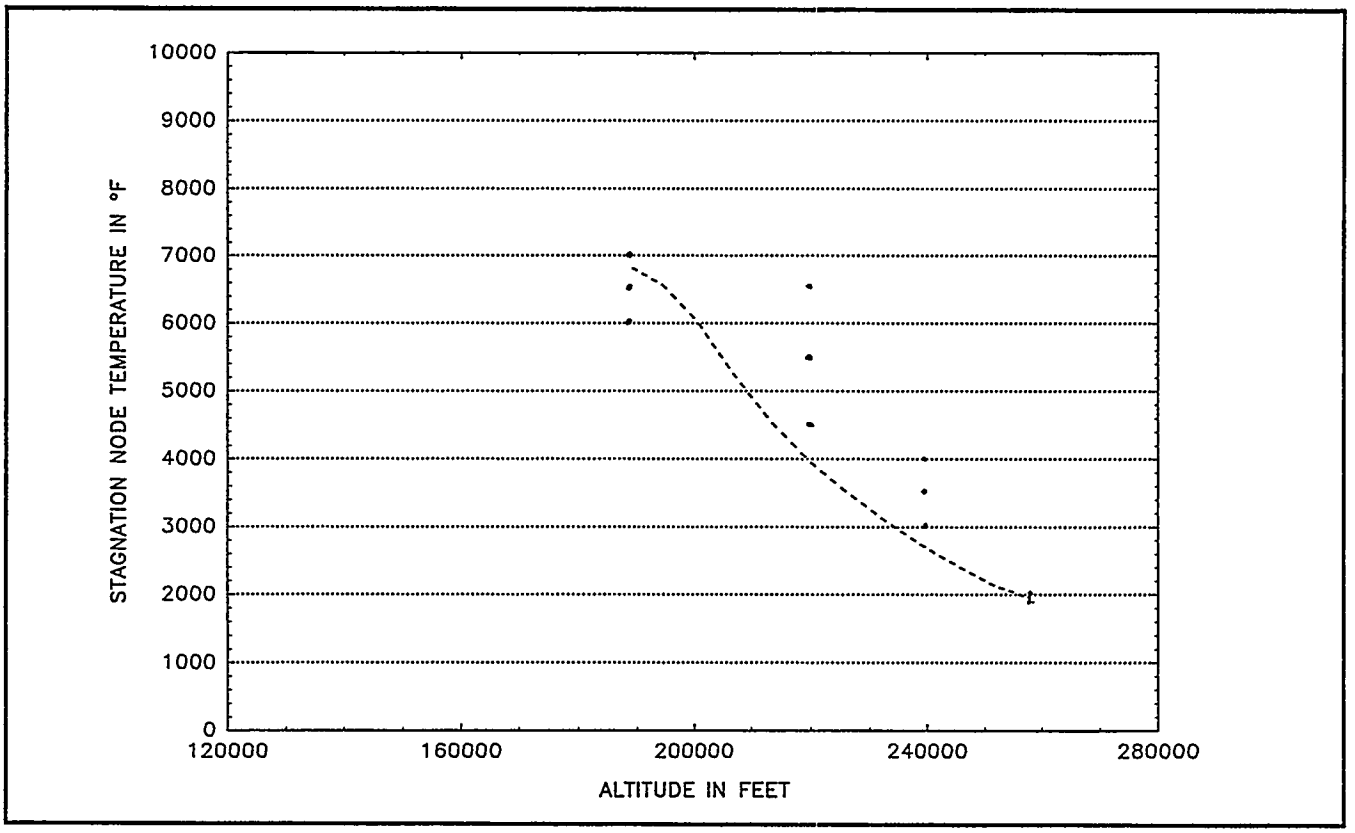

Figure 3-10. Stagnation Node Temperature Vs. Altitude

SINRAP Modification and Documentation: Modifications were made to the SINRAP model to allow for ablation of the innermost aeroshell nodes. This was done to allow for uncertainty runs of the shallow trajectory as well as to allow for the possibility of greater ablation in the steep trajectory. Changes were also performed to incorporate the new CBCF air conductivity model developed by ORNL. A shallow trajectory SINRAP run was made with the added ablation capability. A similar run will be made with both the added ablation capability and the CBCF air conductivity model. These will be compared to the previous SINRAP shallow trajectory run to verify the changes.

The documentation of SINRAP Revision C is underway. This documentation will include a revision of the PIR describing SINRAP (Rev. C) as well as a separate PIR verifying the changes. SINRAP Revision C will include the capability to apply CFD heating and ablation data, the added ablation capability and the updated CBCF air conductivity model.

Reentry Structural Analysis

Shallow Trajectory: The document summarizing the thermostructural analysis for the 7 degree shallow reentry condition completed the review cycle and was issued (*Reference 1*). The thermostructural analysis approach and the results for the shallow trajectory were presented at the 13-14 February INSRP RESP.

Steep Trajectory: Thermostructural analysis was initiated for the steep (90 degree) reentry condition with a face-on stable attitude. The SINRAP transient thermal analysis has progressed through t = 1.1 seconds, which corresponds to an altitude of approximately 188 kft. Data from this analysis was reviewed and cross-plotted with deceleration loads resulting from the 6 DOF runs (see Figure 3-11). As a result, the first timepoint for thermostructural analysis was selected at t = 1.1 seconds, which corresponds to the maximum thermal gradient through the main ablating surface of the aeroshell.

Load conditions at this timepoint are summarized in Table 3-4, and demonstrate some major differences with the loads previously analyzed for the shallow trajectory. The acceleration loads at this altitude (88.8 G's) are already more than 30% higher than the peak acceleration loading for the shallow trajectory, but less than 10% of the maximum value that will be experienced later in the steep trajectory. The peak temperature of 6867°F at this altitude is approximately the same as the highest temperature obtained on the shallow trajectory, but the gradient through the forward face is much steeper, reaching a maximum value of approximately 3750°F, due to the lack of time for thermal penetration on this trajectory. Temperature contours for the aeroshell at t = 1.1 seconds are plotted in Figure 3-12. Though stresses induced by differential thermal expansion will be much higher for the steep trajectory as a result, this condition will be somewhat offset by the presence of cooler, stronger material on the inner surface of the aeroshell. It is also important to note that no significant ablation has occurred at this early point in the steep trajectory.

Preliminary results for the first timepoint of the steep trajectory indicate aeroshell survival at this altitude, with minimum factors of safety in stress and strain of approximately 1.08 and 1.97, respectively. These minima are concentrations located on the outer aeroshell surface in the region of the lock member cutout, and factors of safety elsewhere in the aeroshell are somewhat higher. As has been stated in previous reports, the strain factor of safety is the

critical determinant for aeroshell structural survivability. Thermostructural results for this altitude will be finalized, and analysis of the next timepoint will begin when further results from the CFD/SINRAP analyses become available.

Uncertainty/variability analysis work was initiated with the creation of material databases for use in the uncertainty/variability analyses. Mechanical material properties are the most significant contributors of uncertainty to the thermostructural reentry analysis. In order to quantify the contribution of uncertainty to factors of safety in planned uncertainty calculations, two additional material property databases will be created for the FWPF material. These databases will be of the same form as the nominal material property database created for the baseline analyses, but will represent a correlated set of "high" and "low" properties. The deviation in the data sets from the nominal will be based on the standard deviations obtained from the SoRI test data upon which the nominal properties are based, with extrapolations to higher temperatures where test data is not available.

Table 3-4. Summary of Load Cases for Cassini GPHS Aeroshell - 90° Trajectory

Analysis Time (Secs)	1.1
Altitude (kft)	188.1
Flight Condition	Maximum Gradient
GPHS Weight (lbs)	3.16
Accel. Load (Gs)	88.8
Stagnation Pt. Data	
Temperature	6867
Gradient (°F)	3749
Ablation (in)	0.0012

Reference 1. Vacek, D.J., "Nonlinear Thermostructural Reentry Analysis of the Cassini GPHS Aeroshell: 7 Degree (Shallow) Reentry Flight Path Angle," Lockheed Martin PIR #U-1VC4-Cassini-110, 01-29-96.

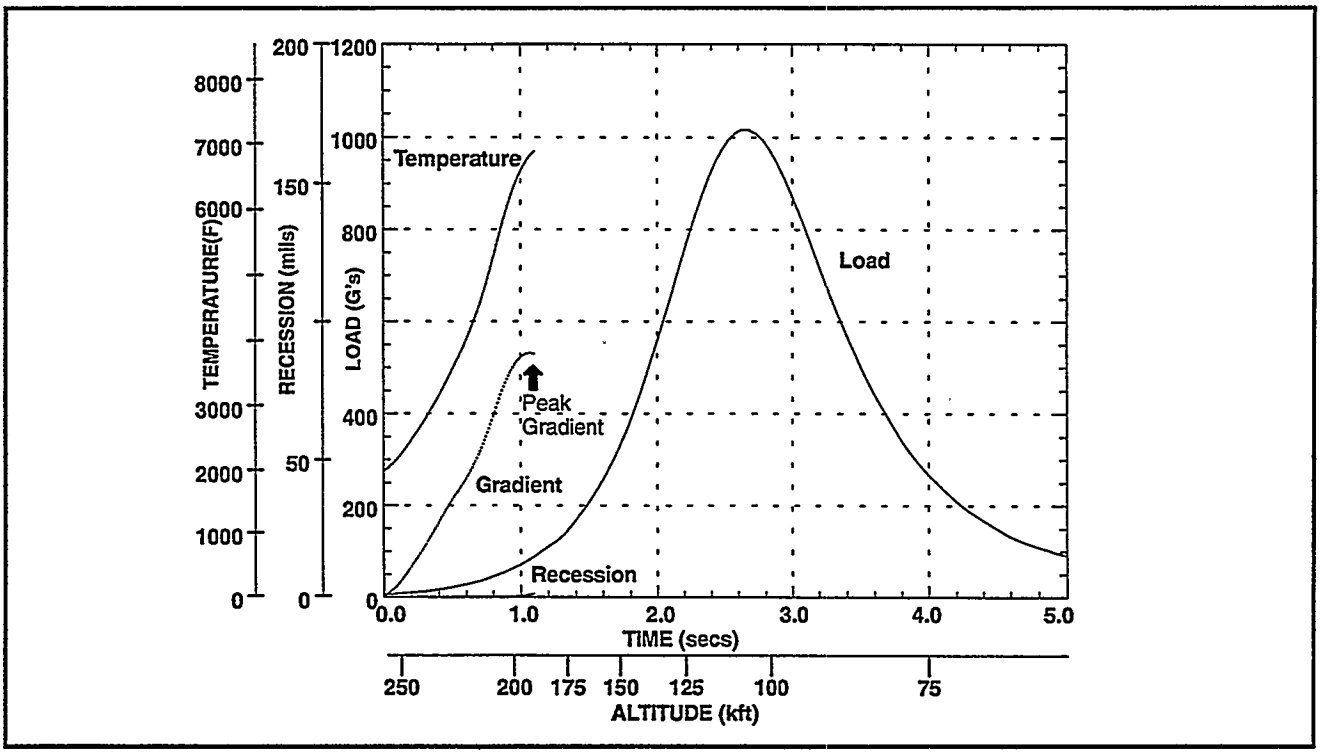

Figure 3-11. Critical Flight Data at Stagnation Point vs. Time - GPHS Aeroshell Cassini 90° Trajectory, Face-On Stable Attitude

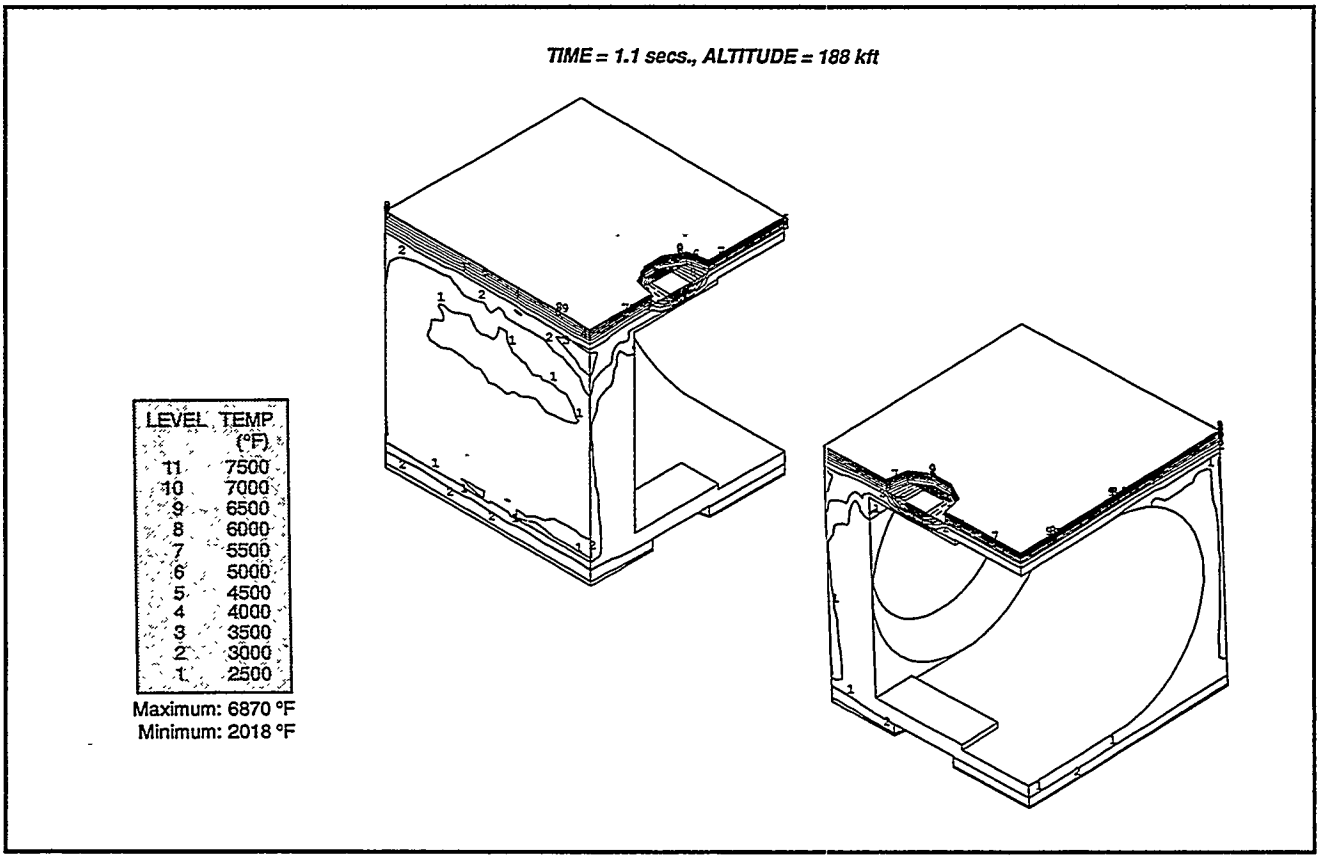

Figure 3-12. Temperature Distribution on Cassini GPHS Aeroshell 90° Trajectory, Face-On Stable Attitude

Variability and Uncertainty

Out-of-Orbit: Out-of-orbit conditions include suborbital reentries, which are the result of an instantaneous loss of thrust in the launch vehicle prior to the attainment of park orbit, reentries due to orbital decay from the normal park orbit, and reentries from off-nominal orbits as result from misdirected or premature termination of the Centaur upper stage second burn. Table 3-5 lists the mean probabilities of occurrence of those Accident Initiating Conditions (AICs) leading to reentry. The corresponding reentry velocity and flight path angle corresponding to these AICs is illustrated in Figure 3-13.

Table 3-5. Accident Initiating Conditions Leading to Reentry

Accident Initiating Condition (AIC)	Mean Event Probability	Comments
Common Core ADS, Conf. 3 & 4	2.84×10^{-3}	Broad Ocean Area Impacts
Thermal Barrier ADS, Conf. 4	7.81×10^{-6}	Broad Ocean Area Impacts
CSDS, Conf. 3	4.05×10^{-5}	Broad Ocean Area Impacts
CSDS, Conf. 4	7.77×10^{-6}	Some Impacts on African Continent
CSDS, Conf. 5	1.15×10^{-2}	Some Impacts on African Continent
Reentry Aeroloading and Heating		
• Suborbital	1.38×10^{-3}	Some Impacts On African Continent
• Nominal Orbital	7.01×10^{-3}	Orbital Decay - World Wide Impacts
• Off-Nominal Orbits, Powered Reentry	3.52×10^{-7}	
• Off-Nominal Orbits, Prompt and Delayed	6.52×10^{-8}	Widespread, nearly world wide impacts
• Off-Nominal Orbits, Elliptical Decayed	8.91×10^{-3}	Orbital decay - world wide impacts

It is assumed that the Aeroshell will survive to impact for all out-of-orbit reentries thus all source terms are derived from surface impacts only. The above assumption is however being established rigorously. The aeroshell maximum recession for all out-of-orbit reentries, with variability and uncertainty, is being determined using a one-dimensional thermal conduction code (REKAP) calibrated with both CFD (computational fluid dynamics) and SINRAP results. Preliminary results indicate that the maximum recession (along the

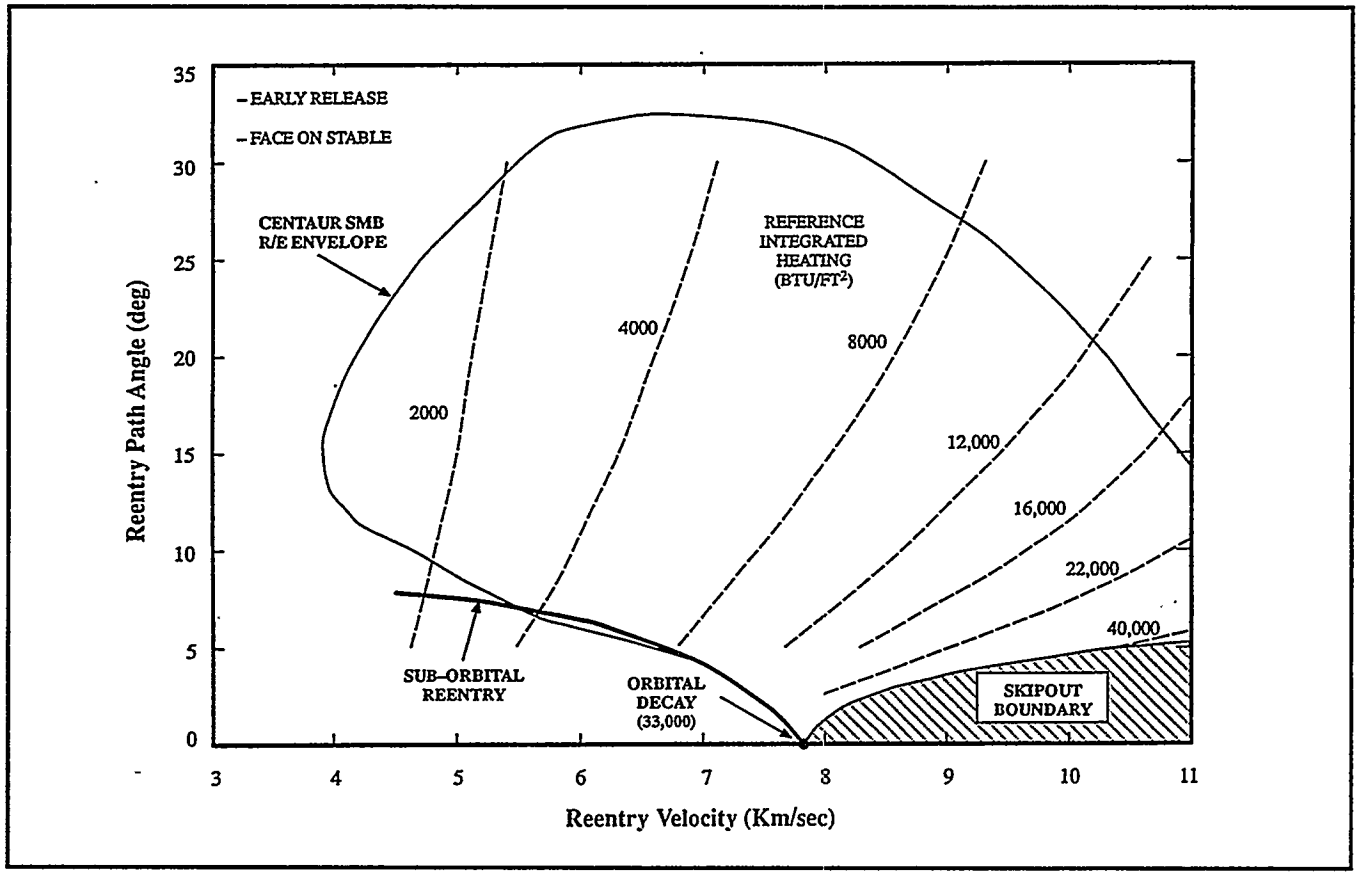

Figure 3-13. Aeroshell Reference Heat Contours

stagnation line), anywhere within the potential reentry envelop, for a face-on-stable orientation is 0.067 inches, occurring at the super-orbital (11 km/s), shallow (just above the skip-out bound) reentry condition. As a point of comparison the recession due to the higher probability reentry from orbital decay is 0.052 inches.

Higher fidelity CFD aerothermal environment (heat flux and mass loss) predictions have been made at the peak heating condition for the orbital decay reentry. Based on these results, it appears that the thermal environment, as predicted by classic empirical/analytical methods as utilized by REKAP, are slightly more severe than the CFD predictions.

Variability in aeroshell ablation predictions for out-of-orbit reentries is provided by atmospheric density (seasonal and latitudinal variation), aeroshell stable orientation (face-on, edge-on, tumbling), reentry velocity and flight path angle, and assessed spacecraft break-up altitude (as determined by JPL). Uncertainty for ablation predictions will result from the aerothermal heating environment predictions, material conduction properties, and mass loss computations.

A Monte Carlo approach is being utilized to determine the surface impact source terms as illustrated in Figure 3-14 specifically for reentries due to orbital decay. In addition to the above variables and parameters this assessment includes the uncertainties associated with the prediction of fuel clad breach and fuel mass/particle size release in exactly the same manner as utilized in the LASEP-T modeling. This is realized by utilizing clad distortion and release subroutines from the LASEP-T model.

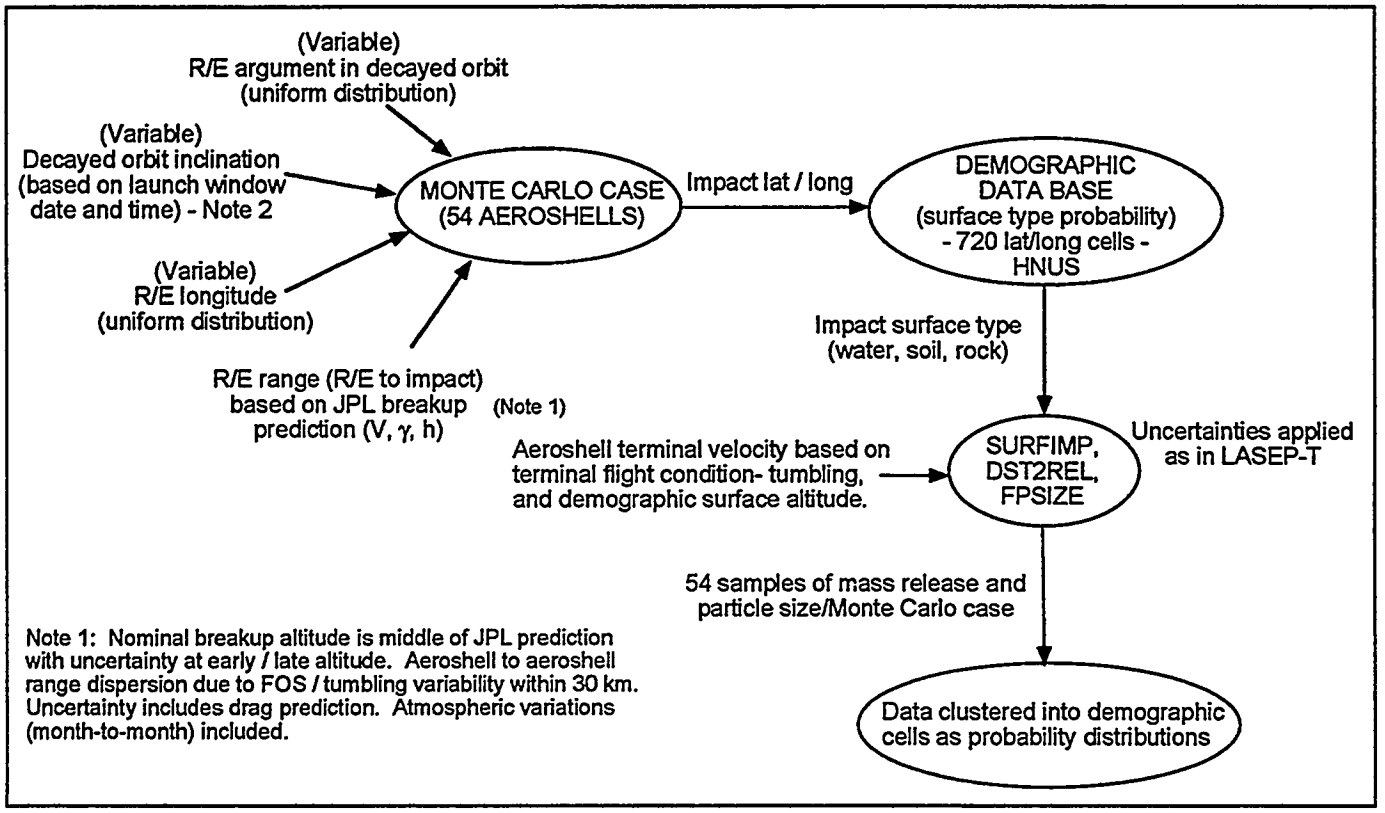

Figure 3-14. Orbital Decay Source Term Methodology

The impact surface type (water, soil, or rock) is determined from a demographic model generated by HNUS which sub-divides the Earth into 720 equal area cells. In addition to surface type this demographic data base includes surface altitude and population. The surface altitude data is used in conjunction with the flight orientation to determine the aeroshell terminal velocity at impact.

Gravity Assist: The basic approach utilized in the assessment of variability and uncertainty for reentries associated with Earth gravity assist fly-by is an event tree. The branches of the event tree (indicating variability) are represented by reentry flight path angle (binned as steep, shallow, and intermediate), atmospheric density (high and low), flight dynamic characteristic (face-on stable or tumbling), aeroshell demise (aerothermal/in-air failure or surface impact), GIS release prediction, and surface type at impact (based on HNUS demographic data).

The uncertainty associated with aeroshell aerothermal/structural failure is being determined based on sensitivity analyses. The sensitivity analysis will provide sensitivity coefficients as well as correlation coefficients between output terms. For in-depth thermal conduction (SINRAP) it may be necessary to also determine interlevel (altitude) influence coefficients to properly correlate the path dependent, non-constant characteristic of parameters.

Uncertainty parameters for the CFD, SINRAP, and ABAQUS models have been identified. Sensitivity analysis for these models is scheduled to begin next month.

Consequence and Risk Analysis

A sensitivity analysis of plume rise and plume diameters was completed using the latest revision of the PUFF model from Sandia National Labs. In this study the energy available for the plume formation was varied over a range of values to simulate fire ball events involving the Titan core or the space vehicle. Five energy levels were used: 1.53E+12, 7.56E+11, 1.53E+11, 3.0E+10, and 1.0E+8 Joules. The first three energy levels were evaluated at 3:00 and 7:00 AM (corresponding to the opening and closing of the daily launch window), while the last two energy levels were evaluated at only 3:00 AM. With 128 October meteorological conditions (one set for each October day between 1987 and 1991), PUFF predicted the cloud stable altitude ranging from 7649 to 87 meters and the cloud diameter ranging from 4256 to 54 meters. In particular, for the case of 7.56E+11 Joules, which is at 50% of the maximum energy level given, the cloud stable altitude reached between 3460 to 825 meters and the cloud diameter ranged from 3894 to 552 meters. The approach to establish the available energy to contribute to plume rise is still under investigation. Through this exercise, the PUFF model has demonstrated the cloud rise and diameter variability that is inherent of the site meteorological conditions and the effects of available energy level.

Interactions with JPL continued for the evaluation of spectator, visitor and worker populations that can be expected for a nighttime Titan launch. A hard copy of a 1994 database for worker populations at KSC and CCAS was obtained. An electronic copy was requested to allow comparison with the currently available 1988 version of this database. This comparison is needed to assure that the 1988 distribution is still adequate and can be scaled to the current totals.

New KSC meteorological data for the periods of November 1990-1994 and October 1992-1994 were received from HNUS. A first step conversion to binary format was performed for all transferred data files and a screening verification was initiated. Due to schedule constraints, meteorological characteristics, such as wind speed, direction and persistence, are currently being analyzed to help narrow the days of November which can contribute relevant additions to the existing database. (As noted above, the existing database covers five years of October data from 1987-1991). For each day of interest, subsequent tasks will involve the generation of the interpolated wind field and related dispersion characteristics.

A first version shell script designed for the automation of SPARRC execution during variability/uncertainty analysis was generated. The process includes reading LASEP-T outputs, generating SATRAP/GEOTRAP input files, execution of applicable codes and storage of results. Linkage with PUFF for plume rise calculation and transfer between SATRAP and GEOTRAP were implemented. Early testings of the shell script has provided various insights regarding file handling and data characteristics, as well as execution time during a large volume analysis.

To improve the running time, several options were implemented in the dose calculation process:

1) For de-minimis dose calculation, the user can set the code to check only a number of years less than the total exposure time interval if the inventory is small. In general, an examination of the first 10 years would be sufficient for a 50 year exposure.

2) De-minimis calculation can be bypassed and re-computed as needed for individual cases. This option would speed up the uncertainty analysis which requires a very large number of cases.

3) Ingestion doses from common food production can be also bypassed if determined negligible a priori.

Safety Test Program

The edge-on fragment engineering test was successfully completed on 6 February 1996. The test consisted of propelling the aluminum test fragment into a stationary converter containing a dummy heat source which was heated to approximately 1090°C. The purpose of the test was to demonstrate that the required fragment velocity (1000 fps), fragment impact accuracy (± 1/4") and heat source impact temperature (1090°C) could be achieved. The test demonstrated that all objectives were met. The test resulted in significant damage to the converter housing and sufficient damage to the dummy heat source (POCO with moly mass) to justify testing the simulated heat source test article (FWPF with fuel simulant). The edge-on fragment test with simulated heat source (test article TA-1) is scheduled to be conducted on 28 February.

TASK 4 QUALIFIED UNICOUPLE FABRICATION

The remaining efforts in Task 4 are associated with testing of 18 couple modules. Test temperatures and life test hours are shown in Table 4-1.

Table 4-1. Test Temperatures and Life Test Hours

Module	Unicouple Source	Test Temperature Hot Shoe	Status as of 25 February 1996
18-10	Early Qualification Lot	1135°C	10,400 hours Performance Normal Test Terminated October 1994
18-11	Full Qualification Lot	1135°C	17,473 Hours Performance Normal
18-12	Early Flight Production Lot	1035°C	13,282 Hours Performance Normal

18 Couple Module Testing

Two modules remain on life test. Testing of module 18-10 was terminated at the end of October 1994 after 10,400 hours.

Module 18-11 (1135°C)

On 25 February 1996, the module reached 17,473 hours at the accelerated hot shoe temperature of 1135°C. Measured performance during this period continues to fall within the data base established by MHW and GPHS 18 couple modules.

The thermoelectric performance evaluation primarily studies the trends of the internal resistance and power factor. Figures 4-1 and 4-2 show these trends in comparison to module 18-8, the last module built during the GPHS program. Agreement is excellent and provides a high degree of confidence that the GPHS unicouple manufacturing processes have been successfully replicated. Table 4-2 summarizes the initial and 17,473 hour performance data.

The isolation resistance trend between the thermoelectric circuit and the foil is shown in Figure 4-3 with modules from the MHW and GPHS programs. The isolation resistance plateaued at about 1000 ohms between 6,000 and 7,000 hours. It then started a slow decrease and is presently at 537 ohms. A similar plateau and gradual decline were observed in MHW module SN-1. At the accelerated temperature of 1135°C the same amount of sublimation occurs in about 1,650 hours of testing as would occur in a 16-year Cassini mission.

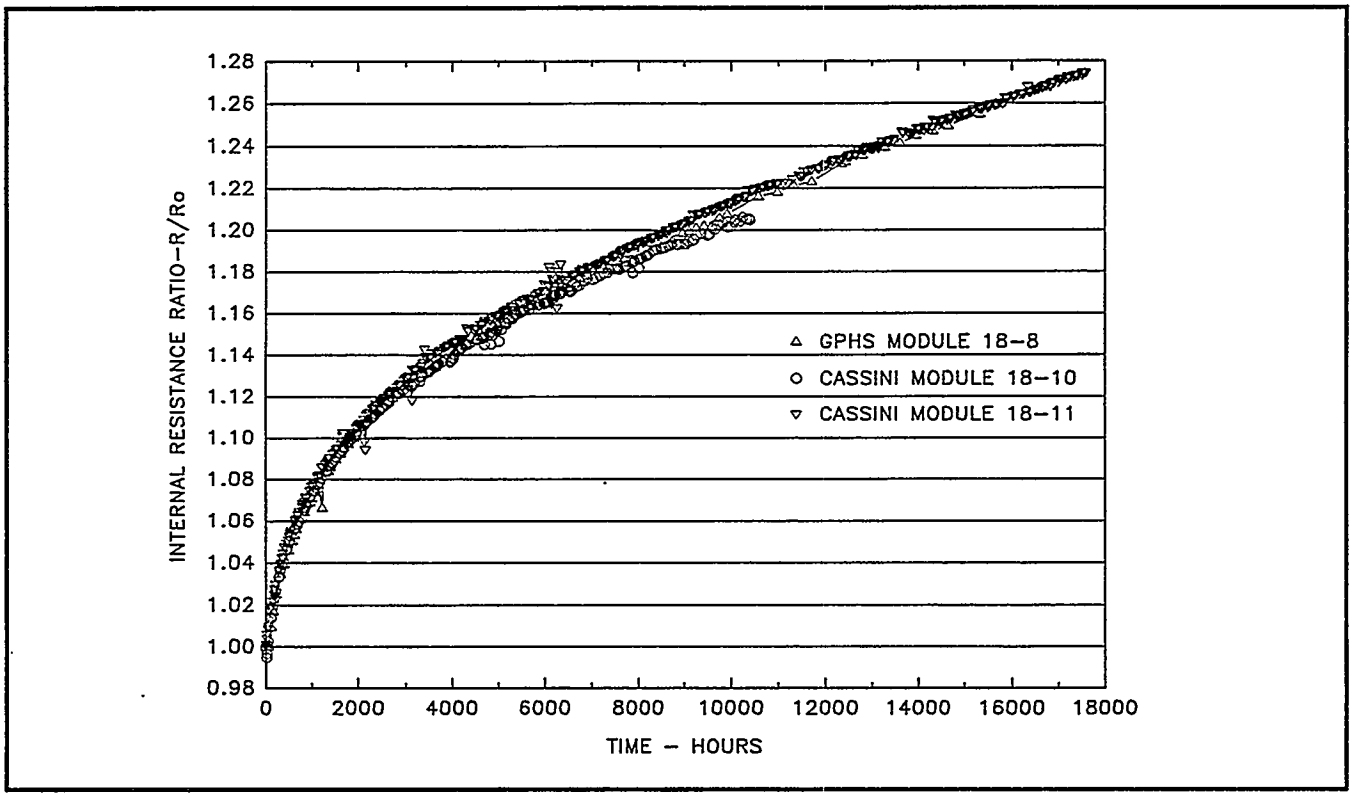

Figure 4-1. Internal Resistance Ratio Versus Time (Modules 18-10, 18-11, GPHS Module 18-8) – 1135°C Operation

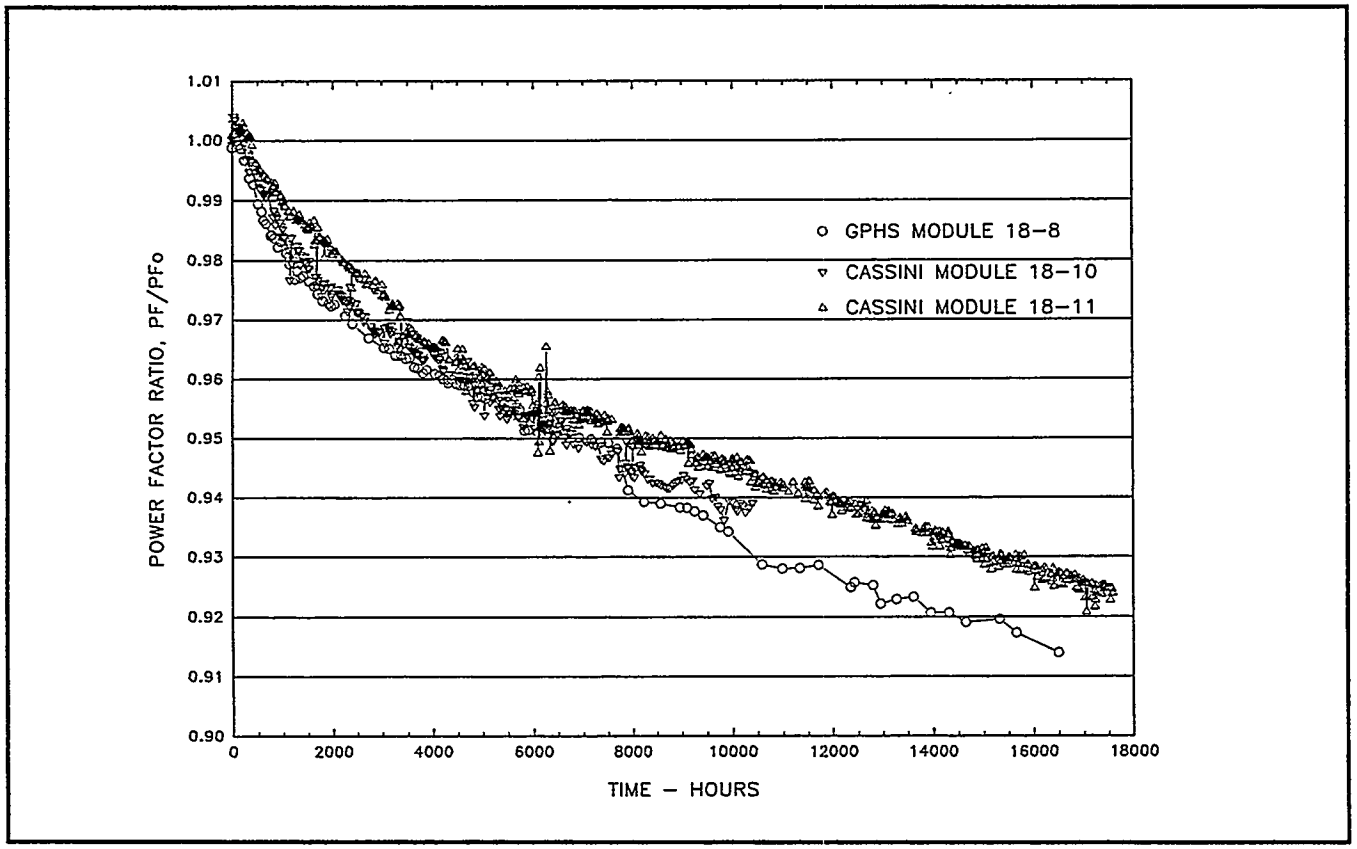

Figure 4-2. Power Factor Ratio Versus Time (Modules 18-10, 18-11, GPHS Module 18-8) – 1135°C Operation

Table 4-2. Comparison of Initial and 17,473 Hour Performance of Module 18-11 at 1135°C

	Initial 2/2/94	t = 52 hours V_L = 3.5V 2/4/94	t = 17,473 hours 2/25/96
Heat Input, Watts	190	192.9	192.6
Hot Shoe, °C Average	1137.8	1137.5	1106.8
Hot Shoe Range °C	5.4	5.2	9.1
Cold Strap, °C Average (8 T/Cs)	311.9	314.3	305.9
Cold Strap Range (8T/Cs)	2.6	2.5	1.9
Cold Strap Average (12 T/Cs)	306.5	308.9	300.9
Cold Strap Range (12 T/Cs)	20.1	20.3	18.6
Load Voltage, Volts	3.895	3.499	3.494
Link Voltage, Volts	0.108	0.121	0.097
Current, Amps	2.842	3.174	2.781
Open Circuit Voltage, Volts	7.140	7.160	7.503
Normalized Open Circuits (8T/Cs)	6.319	6.359	6.857
Normalized Open Circuits (12 T/Cs)	6.276	6.316	6.813
Average Couple Seebeck Coefficient (12)	498×10^{-6}	501×10^{-6}	540.7×10^{-6}
Internal Resistance, Ohms	1.104	1.115	1.407
Internal Resistance Per Couple (Avg.)	0.0613	0.0620	0.0781
Power Measured, Watts (Load + Link)	11.375	11.492	9.99
Power Normalized, Watts (8 T/Cs)	8.909	9.065	8.34
Power Normalized, Watts (12 T/Cs)	8.789	8.942	8.24
Power Factor	40.452×10^{-5}	40.557×10^{-5}	37.41×10^{-5}
Isolation			
Circuit to Foil, Volts	-1.68	-1.36	-1.67
Circuit to Foil, Ohms	6.29K	5.95K	0.54K

Consequently, approximately 10.6 times as much sublimation has occurred during the test duration of module 18-11 as will occur during the Cassini mission. The module performance, therefore, confirms the adequacy of the silicon nitride coating on the qualification couples.

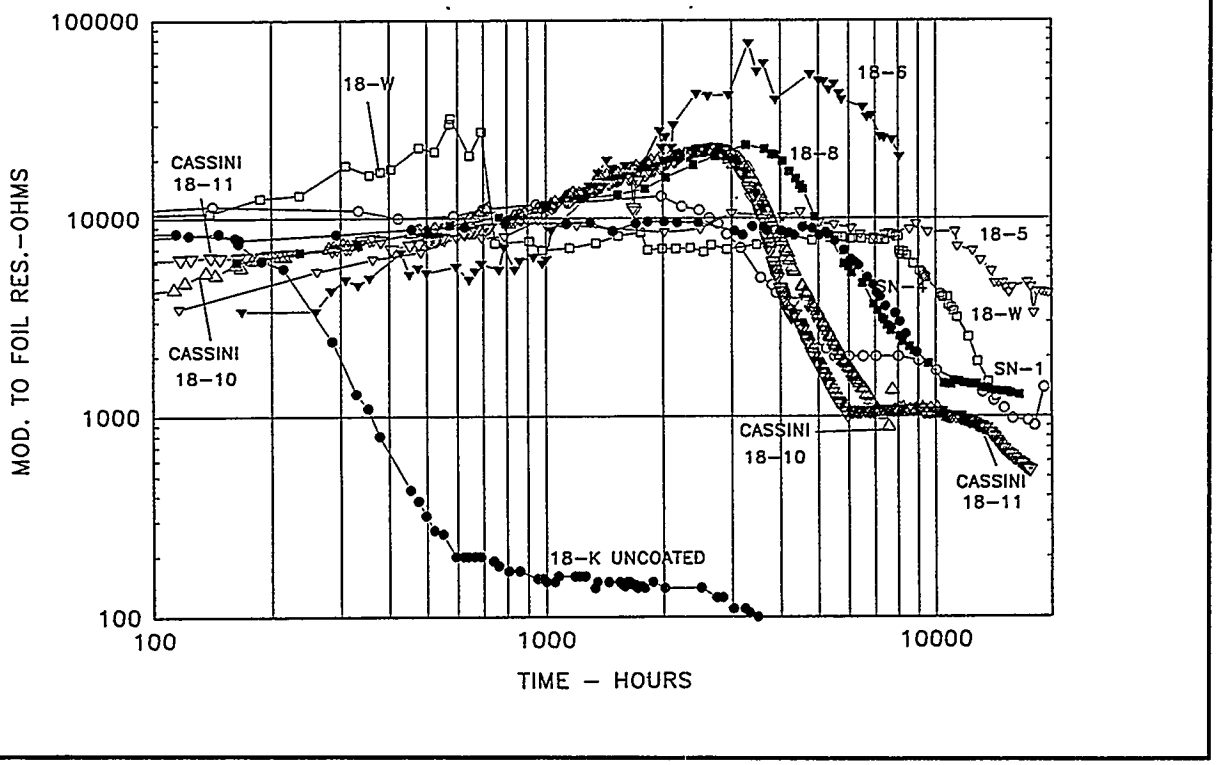

Figure 4-3. Isolation Resistance – Module Circuit to Foil (Modules 18-10, 18-11, GPHS Module 18-8) – 1135°C Operation

Individual Unicouple Performance:

The performance of individual unicouples and rows of unicouples continues to be observed. Table 4-3 shows the room temperature resistance changes and the internal resistance changes observed during operation for each of the six rows and for individual unicouples in Rows 2 and 5. The unicouples continue to perform within a narrow band.

Module 18-12 (1035°C Operation)

The module reached 13,282 hours at the normal operating temperature of 1035°C on 25 February 1996 . Thermoelectric performance, as measured by internal resistance and power factor trends, continues to be normal as shown as Figures 4-4 and 4-5, respectively. Table 4-4 shows initial performance and the performance on 25 February 1996.

Isolation Resistance

The isolation resistance between the circuit and foil continues to show the normal trend as shown in Figure 4-6.

Individual Unicouple Performance

A review of the unicouple internal resistances and open circuit voltages indicates that all unicouples are exhibiting very similar behavior with time (See Table 4-5). The data for the six individually instrumented unicouples in Rows 2 and 5 are shown in Figure 4-7.

Table 4-3. Module 18-11 Internal Resistance Changes

Position	Serial #	2nd Bond Milliohm	Preassy Milliohm	Delta ri Milliohm	T = 0 Milliohm	T=1,509 Hours	Delta ri Milliohm	Percent Increase	T=17,473 Hours	Delta ri Milliohm	Percent Increase
1.0	H2006	22.50	22.10	-0.40							
2.0	H0507	22.40	21.90	-0.50							
3.0	H0512	22.7	22.20	-0.50							
					182.30	199.70	17.40	9.54	233.30	51.00	28.00
4.0	H0439	23.20	22.70	-0.50	62.30	67.90	5.60	8.99	79.10	16.80	27.00
5.0	H0587	22.50	22.40	-0.10	61.00	66.50	5.50	9.02	77.10	16.10	26.40
6.0	H0657	22.70	22.50	-0.20	61.40	67.30	5.90	9.61	78.40	17.00	27.70
					184.10	201.10	17.00	9.23	233.80	49.70	27.00
7.0	H0585	22.90	22.50	-0.40							
8.0	H0459	22.50	22.10	-0.40							
9.0	H0562	22.70	22.30	-0.40							
					185.70	203.20	17.50	9.42	237.80	52.10	28.10
10.0	H0248	22.70	22.30	-0.40							
11.0	H0163	22.90	22.40	-0.50							
12.0	H0282	22.70	22.40	-0.30							
					184.90	201.70	16.80	9.09	233.90	49.00	26.50
13.0	H0428	23.10	22.70	-0.40	62.10	67.90	5.80	9.34	78.90	16.80	27.10
14.0	H0326	22.60	22.00	-0.60	62.20	68.30	6.10	9.81	80.00	17.80	28.60
15.0	H0232	22.60	22.00	-0.60	60.90	66.60	5.70	9.36	78.20	17.30	28.40
					184.70	202.30	17.60	9.53	236.50	51.80	28.00
16.0	H0590	22.60	22.40	-0.20							
17.0	H0393	22.60	22.10	-0.50							
18.0	H0496	22.50	22.30	-0.20							
					184.20	201.40	17.20	9.34	233.60	49.40	26.80

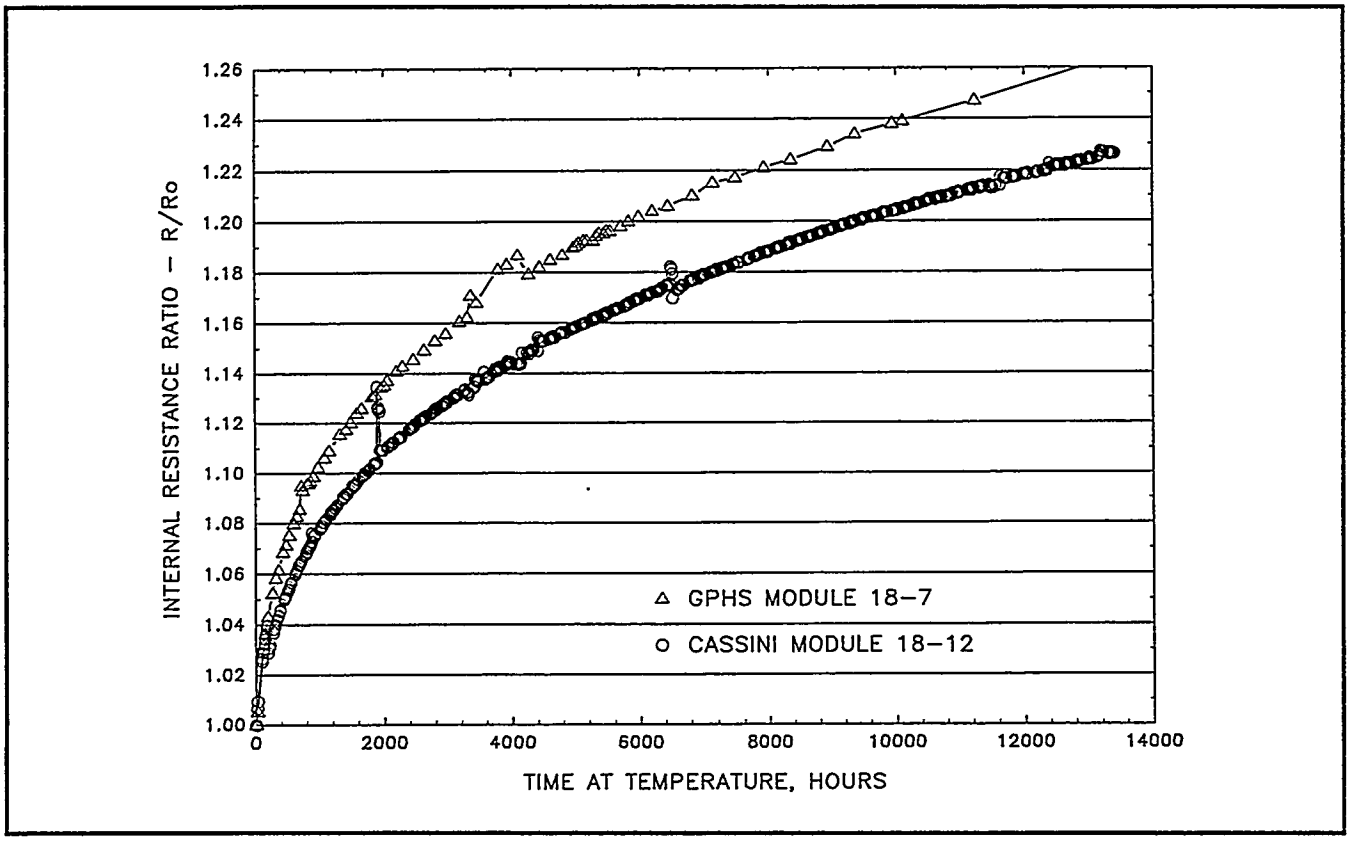

Figure 4-4. Internal Resistance Ratio Versus Time (Modules 18-12, and 18-7) – 1035°C Operation

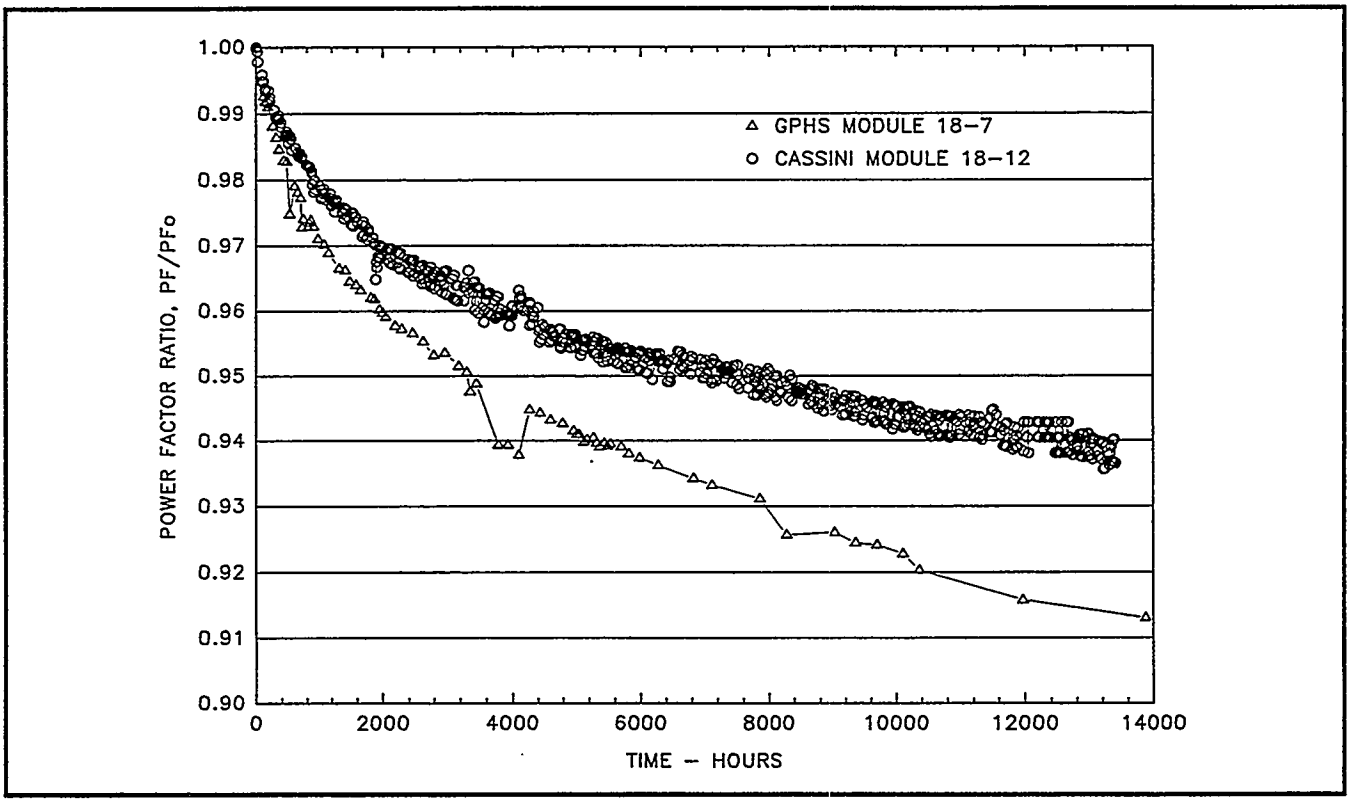

Figure 4-5. Power Factor Ratio Versus Time at Temperature (18-7 and 18-12) – 1035°C Operation

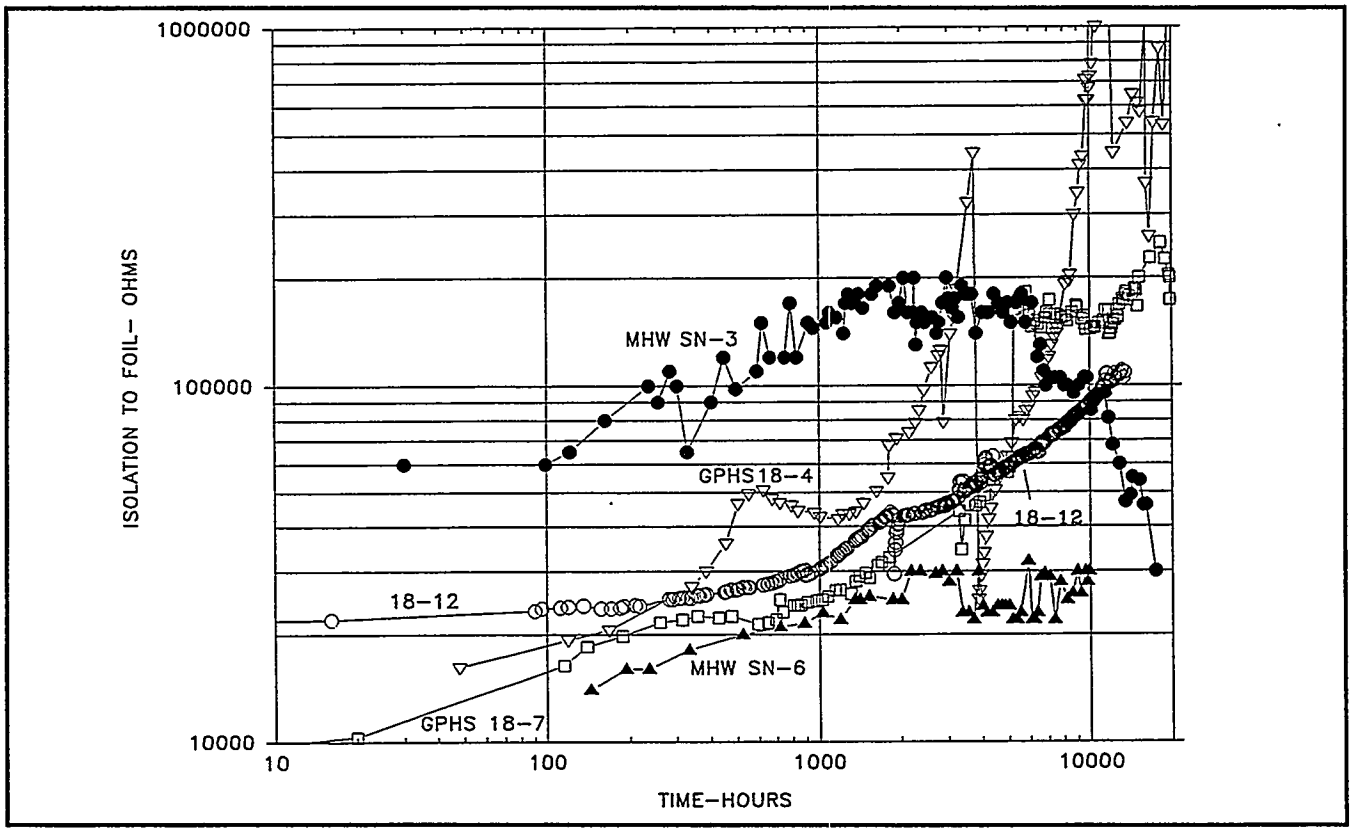

Figure 4-6. Isolation Resistance – Module Circuit to Foil (18-12, GPHS and MHW Modules) – 1035°C Operation

Table 4-4. Comparison of Initial and 13,282 Hour Performance of Module 18-12 at 1035°C

	Initial 6/16/94	t = 13,282 Hours 2/25/96
Heat Input, Watts	169.15	169.7
Hot Shoe, °C Average	1035.9	1028.6
Hot Shoe Range °C	5.7	4.5
Cold Strap, °C Average (8 T/Cs)	287.1	282.4
Cold Strap Range (8T/Cs)	5.0	5.0
Cold Strap Average (12 T/Cs)	282.7	278.1
Cold Strap Range (12 T/Cs)	19.8	19.5
Load Voltage, Volts	3.578	3.498
Link Voltage, Volts	0.155	0.154
Current, Amps	2.548	2.473
Open Circuit Voltage, Volts	6.431	6.863
Normalized Open Circuit (8T/Cs)	6.307	6.755
Normalized Open Circuit (12 T/Cs)	6.268	6.714
Average Couple Seebeck Coefficient (12)	497×10^{-6}	532.9×10^{-6}
Internal Resistance, Ohms	1.053	1.299
Internal Resistance Per Couple (Avg.)	0.0588	0.0721
Power Measured, Watts (Load + Link)	9.510	9.03
Power Normalized, Watts (8 T/Cs)	9.146	8.75
Power Normalized, Watts (12 T/Cs)	9.011	8.64
Power Factor	42.06×10^{-5}	39.36×10^{-5}
Isolation		
Circuit to Foil, Volts	-1.71	-0.85
Circuit to Foil, Ohms	21.3K	107.5K

Table 4-5. Module 18-12 Internal Resistance Changes

Position	Serial #	2nd Bond Milliohm	Preassy Milliohm	Delta ri Milliohm	T = 0 Milliohm	T=1,505 Hours	Delta ri Milliohm	Percent Increase	T=13,282 Hours	Delta ri Milliohm	Percent Increase
1.0	H2594	23.80	22.90	-0.90							
2.0	H2634	22.70	22.60	-0.10							
3.0	H2606	23.50	22.40	-1.10							
					176.80	192.10	15.30	8.65	214.60	37.80	21.40
4.0	H2168	22.20	21.70	-0.50	57.50	63.30	5.80	10.09	71.40	13.90	24.20
5.0	H2151	22.40	21.90	-0.50	57.40	62.90	5.50	9.58	70.60	13.20	23.00
6.0	H2256	22.20	21.70	-0.50	57.00	63.10	6.10	10.70	71.40	14.40	25.30
					171.20	188.60	17.40	10.16	212.60	41.40	24.20
7.0	H2597	24.40	23.20	-1.20							
8.0	H2680	22.60	23.00	0.40							
9.0	H2658	22.70	23.00	0.30							
					178.00	193.60	15.60	8.76	216.10	38.10	21.40
10.0	H1506	23.50	23.20	-0.30							
11.0	H1392	23.80	23.00	-0.80							
12.0	H1606	23.60	22.60	-1.00							
					176.20	193.40	17.20	9.76	216.80	40.60	23.00
13.0	H1344	23.60	23.50	-0.10	59.20	64.80	5.60	9.46	72.50	13.30	22.50
14.0	H1618	23.30	24.00	0.70	58.60	64.50	5.90	10.07	72.60	14.00	23.90
15.0	H1262	23.70	23.30	-0.40	59.40	65.00	5.60	9.43	72.80	13.40	22.60
					176.60	193.70	17.10	9.68	217.20	40.60	23.00
16.0	H1580	23.00	23.70	0.70							
17.0	H2127	22.80	22.10	-0.70							
18.0	H2113	22.90	22.20	-0.70							
					174.50	191.30	16.80	9.63	214.70	40.20	23.00

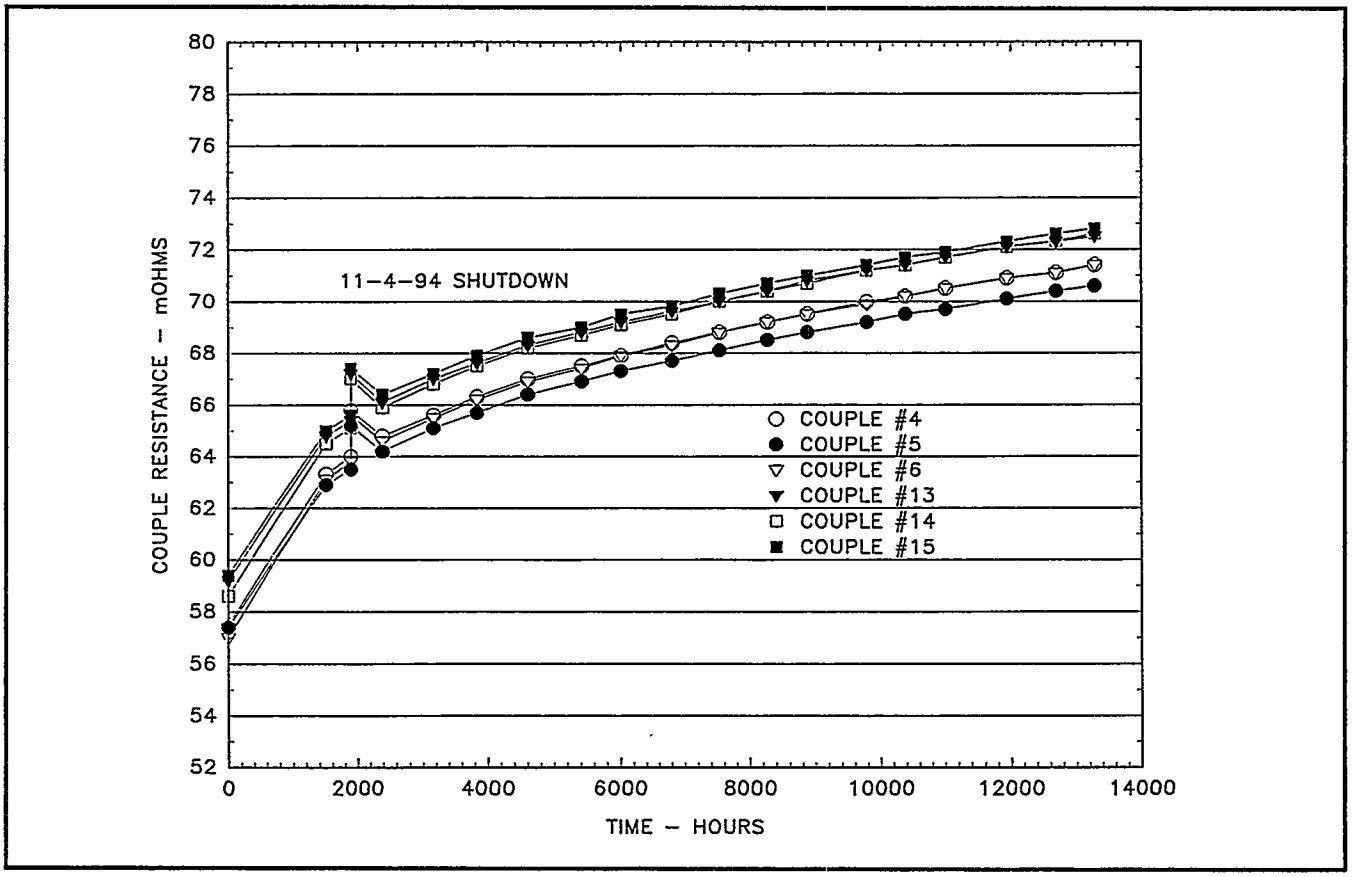

Figure 4-7. Individual Unicouple Internal Resistance Trends (Module 18-12)

TASK 5 ETG FABRICATION, ASSEMBLY, AND TEST

E-6 ETG Test Activity (Building 800)

The E-6 ETG continues in storage in Building 800. ETG and Converter Shipping Container (CSC) pressures are being monitored and adjusted, as required, to maintain storage pressure requirements.

E-7 Processing and Testing

At the end of the last reporting period the ETG had a heat input of approximately 3200 watts. Normal heat-up continued from that point at a rate of approximately 10 watts/hour until reaching full power at 4415 watts on 1 February. All vacuum requirements for both the ETG and the LAS were satisfied throughout processing.

After completion of a 24 hour "soak" period, the EHS input power was reduced to 4402 watts. Stabilization was achieved and a 76 hour performance test was started. Thermopile circuit resistance to ground at beginning of the 24 hour "soak" period was 5.6 K ohms. At the beginning of the 76 hour performance test the resistance had decreased to 3.5 K ohms and continued to decrease. At 21 hours into the test the resistance was 2.71 K ohms. At that time it was decided to reduce the EHS heat input to 4258 watts (the expected Cassini fuel loading). The resistance increased to 3.4 K ohms and then started to decrease at a rate similar to the rate observed for the 4402 watt heat input. At 36 hours into the test the heat input was further reduced to 4000 watts. RGA data showed mass numbers 2, 18, 28 and 78 were significantly less than at full heat input, indicating a reduction in the outgassing rates. The total ETG pressure also continued to decrease. A decision was made at that time to reduce the heat input to 2900 watts and backfill the LAS with argon gas. The argon gas backfill occurred on 5 February and the ETG was stabilized at a heat input of 4400 watts. The heat input of 4400 watts in argon results in hot side temperatures similar to 2900 watts under vacuum conditions.

On 6 February, the LAS was re-evacuated and stabilized under vacuum conditions at a heat input of 2900 watts. The ETG performance data was compared to the previous heat up cycle at 2900 watts heat input and found to be

in good agreement. Heat inputs were restarted at approximately 10 watts/hour and continued until a loss of vacuum was experienced on 7 February. The backfill was completed and the ETG re-stabilized at 4400 watts. The loss of vacuum was caused by a leak in the LN_2 line which resulted in LN_2 dripping onto the turbo molecular pump cold trap and warping the cover plate. All the hi-vac valves closed automatically, however, blue discoloration was noted on the ETG outboard pre-load frame.

The LN_2 leak was repaired and baffles installed to prevent a reoccurrence. The LAS was re-evacuated on 8 February. The EHS heat input was re-stabilized at 2900 watts. The ETG performance data was again compared to previous data with stabilized heat input at 2900 watts and found to be in good agreement, indicating no adverse effects from the loss of vacuum and argon backfill. On 9 February, the RGA filament burned out, thereby shutting down the RGA. Heat input continued at 10 watts/hour providing that all pressure requirements were satisfied. The total ETG pressure was approximately one decade less than the specification and one decade less than during the initial heat up cycle. On 13 February, the heat input was approximately 3800 watts and the ETG pressure continued to slowly increase. The heat input rate was reduced to 5 watts/hour until 14 February, when the thermopile circuit to case resistance was 3.29 K ohms and the ETG pressure was 9.8×10^{-6} torr. Heat input increases were halted for 7 hours to verify that the ETG pressure and thermopile circuit to case resistance would stabilize. The heat input at this time was 4090 watts. Within a few hours both the resistance and pressure stabilized, and direction was given to resume heat inputs at 5 watts/hour. Heat inputs continued at this rate until the full heat load of 4402 watts was achieved on 17 February except for a short hold at 4300 watts to again verify stability.

A second stability test at 4402 watts was started on 17 February. The ETG thermopile circuit to case resistance was 1.69 K ohms and the ETG partial pressure was 1.7×10^{-5} torr at the beginning of the 76 hour stability test. The ETG performance data remained fairly constant through approximately 26 hours of testing and at this point the ETG pressure started to increase and the

thermopile circuit to case resistance began to decrease (in 5 hours it decreased to 1.4 K ohms). At 30 hours into the test, the EHS power input was reduced to 4300 watts and the pressure and isolation resistance stabilized. At 36 hours into the test, a further EHS reduction was made to 4100 watts. The ETG pressure decreased to 1.6×10^{-5} torr at 38 hours into the test and the isolation resistance increased to 2.35 K ohms. The 4100 watt input was maintained while awaiting MRB direction. Even though the acceptance requirement at full heat input is 1 KΩ, Lockheed Martin recommended cessation of full heat input vacuum testing with the installed EHS so as not to further degrade the isolation resistance. Based on a review of previous units including Q-1 which utilized this same EHS, the most likely cause of the decreased isolation resistance is effluent gases from the EHS. In Q-1, this decrease was reversed after fueling with the isotope heat source.

NR 79348 documented the problem experienced and was dispositioned to proceed to the capacitance test. This test was initiated on 19 February and was performed in accordance with SI No. 252256. Capacitance measurements were made with heat inputs of 4100, 3800, 3500 and 3200 watts. The testing was done at short circuit voltage for all power levels and at open circuit voltage for 3500 watts. After completion of the testing, the ETG was re-stabilized at 30 volts load. Direction was received from MRB to complete all remaining acceptance testing, and install the ETG into the converter shipping container. The LAS was backfilled with argon gas on 21 February and the ETG stabilized with a heat input of 4402 watts. The 4 hour performance test was completed. All ETG performance requirements were satisfied except for the 76 hour stability test duration. The ETG performance summary is presented in Table 5-1.

The performance data were reviewed and accepted by Engineering and Product Assurance personnel. Approval was give to initiate EHS power down in preparation for outboard dome and midspan cap installation. The EHS power reduction was completed on 22 February.

Table 5-1. E-7 ETG Performance Testing

	Initial Stability Test		Second Stability Test		Argon Performance Test	
Test Duration – Hours	T_o	T + 21	T_o	T + 30	T_o	T + 4
EHS Power – Watts	4400	4401	4402	4403	4402	4404
ETG Power[1] – Watts	296.3	295.6	294.6	294.6	158.1	158.8
RTD Temperature – °C	252	252	252	252	183	183
Load Voltage – Volts	30.0	30.0	30.0	30.0	30.0	30.0
Load Current – Amps	9.8	9.8	9.8	9.8	5.3	5.3
Open Circuit Voltage – Volts	50.7	50.8	51.4	51.4	40.7	40.7
Internal Resistance – Ohms	2.11	2.12	2.19	2.19	2.03	2.03
R Shunt Case – K Ohms	3.5	2.7	1.7	1.4	84	78
ETG Pressure – Torr	$3.7E^{-5}$	$2.7E^{-5}$	$1.7E^{-5}$	$2.4E^{-5}$	15 psi	15 psi
ETG Acceptance Requirements						
ETG Power – Watts	293 (Minimum)		293 (Minimum)		130 (Minimum)	
R Shunt Case K Ohms	1.0 (Minimum)		1.0 (Minimum)		1.0 (Minimum)	

[1] Corrected to Connector Pins

Installation of the outboard pressure dome was completed without incident on 23 February. Midspan cap installation was also completed on the same day. The ETG was then pressurized to begin pressure decay testing, however, it was quickly apparent the ETG was leaking excessively due to the rapid loss of ETG pressure.

Based on previous experience, it was believed the most probable cause for the leakage was at the midspan caps. The midspan caps were removed one at a time and passed outside the LAS via the tool lock pass-through. The condition of the o-rings were examined and found acceptable. It was decided, however, to replace the o-rings with new ones and reinstall the midspan caps. This was accomplished but with no significant change in the leak rate. An NR was written

and dispositioned to perform a helium sniff test to identify the leak site once the LAS door was opened. The gas processing valve was closed and the ETG was pressurized to 25 psia via the Gas Service Cart (GSC) and monitored. The ETG pressure immediately stabilized, indicating the leakage was in the LAS plumbing. The ETG was pressurized to 25 psia and a 6 hour cold pressure decay test was performed. No pressure decay was observed over the 6 hour period when corrected for temperature effects. The requirement is that the decay be less than 0.20 psia for 6 hours. The ETG was being prepared for removal from the LAS at the end of the reporting period.

E-8 Converter Hardware

Assembly of the EHS continued with the welding of new leads to the heater elements. Ceramic pieces were machined to meet the drawing and the upper and lower subassemblies were assembled. Forming of the power leads will be performed in the next reporting period.

Boron nitride was applied to the C-seal surfaces of the E-8 shell/fin assembly. The assembly was sent to an outside vendor for vacuum curing. The shell/fin assembly has been returned to Lockheed Martin after completing vacuum bakeout.

A new batch of PD224 paint was mixed after the new silicone resins were delivered and accepted. Testing of the paint samples will be performed in the next reporting period. The shelf life to the new paint batch is one year.

Approximately 100 of the 144 unicouples removed from the E-7 ETG have completed the annealing rework process and are undergoing final inspection. These unicouples will replace the E-8 unicouples which were removed from stock and installed into E-7.

TASK 6 GROUND SUPPORT EQUIPMENT (GSE)

All lifting hardware required for the Trailblazer activity was proof loaded and dye penetrant inspected. The hardware will be shipped to the Cape early next month.

Machining of the first set of brackets for the converter support ring was completed. Assembly of the first converter support ring will be initiated during the next reporting period.

TASK 7 RTG SHIPPING AND LAUNCH SUPPORT

Launch Activity

Lockheed Martin concurred with the revised JPL Trailblazer procedures concerning RTG operations. Preparations continued for shipping the RTG ground support equipment needed for the Trailblazer to the launch facility. Shipment is planned for early next month, in time for the start of Trailblazer which is scheduled for the latter half of the month. Launch facility orientation and training films were being viewed, as requested by JPL-KSC, in preparation for gaining access to the launch complex.

TASK 8 DESIGNS, REVIEWS, AND MISSION APPLICATIONS

8.1 Galileo/Ulysses Flight Performance Analysis

No significant activity this reporting period.

8.2 Individual and Module Multicouple Testing

This task has been successfully completed.

8.3 Structural Characterization of Candidate Improved N- and P-Type SiGe Thermoelectric Materials

This task has been successfully completed.

8.4 Technical Conference Support

No significant activity this reporting period

8.5 Evaluation of an Improved Performance Unicouple

Module 18-Z

This task has been successfully completed.

8.6 Solid Rivet Feasibility Study

This task has been successfully completed.

8.7 Computational Fluid Dynamics (CFD)

Work continues on the CFD task. Because this task is closely related to the Task 3 safety activities, technical progress is reported under that task.

8.8 Technical International Conference Support

This task has been successfully completed.

8.9 Additional Safety Tasks

Additional safety efforts have been assigned to this task. Because these efforts are closely related to the Task 3 safety activities, technical progress is being reported under that task.

TASK 9 PROJECT MANAGEMENT, QUALITY ASSURANCE, AND RELIABILITY

9.1 Project Management

All contractual reports, CDRLs, and milestone documents were delivered on schedule.

Lockheed Martin attended the Cassini quarterly review at OSC in Germantown, MD. Lockheed Martin also attended the INSRP RESP subpanel review in El Segundo, CA, and witnessed the side-on fragment engineering test at Sandia National Laboratories, NM. Technical support was provided during this period at Mound for the assembly of the F-2 RTG.

E-7 processing was completed this reporting period. All performance requirements were met except for the completion of the 76 hour stability test. Efforts to complete the 76 hour test were unsuccessful due to abnormal outgassing within the ETG, believed to be caused by the electric heat source. This resulted in the electrical isolation resistance of the ETG being lower than those of previous ETGs, but still meeting specification requirements. An investigation into the cause of the problem and an assessment of the long term effects, if any, of the lower isolation resistance are underway.

Attached are the Cassini RTG program calendars for 1Q96 and 2Q96 showing program meetings and important related events.

No significant environmental, health, or safety incidents occurred during this period.

9.2 Quality Assurance

Quality Plans and Documents

No plans were initiated or modified during this period.

Quality Control in Support of Fabrication

E-8 Converter: Work on subassemblies for E-8 is continuing. E-8 hardware is being assembled into kits such that it could be fully assembled at some point in the future, if required. In-process inspection support was provided during the preparation of a new batch of PD-224 paint which will be used to coat several E-8 components. Support was also provided for the fabrication of the E-8 electric heat source. No significant problems were noted with E-8 hardware during this period.

Unicouple Production

Effort to upgrade specifications and drawings to accurately describe all processes for future builds has been completed.

Rework of the unicouples removed from E-7 is continuing. Unicouples are being unwrapped, unstuffed, and hydrogen fired to anneal the copper connectors. They will then follow the normal assembly and inspection procedures in preparation for returning them to stock. Approximately 100 unicouples have completed the anneal process. Inspection has revealed some staining of the hot shoe spacers which appears to have occurred during cleaning prior to annealing. This problem has been addressed and the cleaning procedure has been modified to minimize this problem. Other types of defects have been minimal, to date.

E-6 Converter: The E-6 converter remains in the shipping container and is in long term storage in Building 800 until required for processing at Mound. Internal pressure is being monitored on a regular basis and gas is being replenished, as required. The C of I has been conditionally approved by the customer and the DD 250 shipping document has also been approved.

Quality Assurance Audits

There was no audit activity during this reporting period.

Quality Assurance Status Meeting

No general status meetings were held during this reporting period.

TASK H CONTRACTOR ACQUIRED GOVERNMENT OWNED (CAGO) PROPERTY ACQUISITION

Task H.1 CAGO Unicouple Equipment

No significant activity during this reporting period.

H.2 CAGO - ETG Equipment

No significant activity during this reporting period.

H.3 CAGO - MIS

No significant activity during this reporting period.

Cassini RTG Program Calendar

As of 20 March 1996

1st QTR 1996

	M	T	W	T	F	S	S	FW
JANUARY	1 Happy New Year 	2	3 F-2 Paint and Modifications - EG&G Mound - *Reinstrom, et al*	4 Fireball Model - Sandia National Labs - (Albuquerque) *Braun, Chang, DeFillipo*	5	6	7	01
	8	9 Space Technology and Applications International Forum - Albuquerque, New Mexico - Josloff	10	11 *Cassini 5th Anniversary* F-2 Readiness Review - EG&G Mound - *Cockfield, Reinstrom*	12	13	14	02
	15	16	17 INSRP Review - Sheraton Hotel - Valley Forge - *Braun, et al*	18	19	20	21	03
	22	23 Monthly Reports Due to DOE	24	25 F-2 Support - EG&G Mound - *Kugler*	26	27	28	04
FEBRUARY	29	30 Cassini Quarterly Program Review - OSC, Germantown MD - *Hemler, Cockfield, Reinstrom, DeFillipo*	31	1	2 F-2 Support - EG&G Mound - *Cockfield*	3	4	05
	5 F-2 Support - EG&G Mound - *Cockfield*	6 Safety Test Hot Eng. Fragment Test - Albuquerque, New Mexico - *Hartman, Kauffman*	7	8	9	10	11	06
	12 F-2 Support - EG&G Mound - *Kugler*	13	14 INSRP RESP Subpanel Review - El Segundo, CA - *Hemler/Cockfield/ DeFillipo/Tobery/Daywitt/Letts/Vacek*	15 RTG Installation Cart Demo - JPL CA - *Reinstrom/Cockfield*	16 F-2 Support - EG&G Mound - *Kugler*	17	18	07
	19	20	21 Operations Analysis On-Site Visit - EG&G Mound - *Reinstrom*	22	23 Monthly Reports Due to DOE	24	25	08
MARCH	26	27	28 Side-On Fragment Safety Test (TA-1) - Albuquerque, NM - *Hartman/Cockfield*	29	1 Sterling Franks Visit to Bldg. B - Valley Forge, PA - *Hinners/Hemler/et al*	2	3	09
	4	5	6 Full Stack Intact Impact Accident Assessment Plan - Valley Forge, PA - *LMASD/LMMS/DOE et al*	7	8	9	10	10
	11	12 Cassini Monthly Program Review - OSC, Germantown MD - *Hemler, Cockfield, Reinstrom, DeFillipo*	13	14 Cassini Review - JPL CA - *Hemler*	15	16	17	11
	18	19	20	21	22 Monthly Reports Due to DOE	23	24	12
	25 Trailblazer Readiness Review - Cape Canaveral, FL - *Haley/Reinstrom*	26 Side-On Fragment Safety Test (TA-1) - Albuquerque, NM - *Cockfield* SPARRC Variability/ Uncertainty Rev. w/SNL - LMMS - San Jose - *DeFillipo/Kampas*	27	28	29	30	31	13

Trailblazer Activities .....

Cassini RTG Program Calendar

As of 20 March 1996

2nd QTR 1996

	M	T	W	T	F	S	S	FW
APRIL	1	2	3 Pre-Ship Review of E-7 ETG Converter - Valley Forge -	4	5	6	7	14
	8	9	10	11 Cassini Quarterly Program Review - JPL - CA - *Hemler, Cockfield, Reinstrom, DeFillipo*	12	13	14	15
	15	16	17	18	19 Semi-Annual Reports Due to DOE	20	21	16
	22	23 Monthly Reports Due to DOE	24	25	26	27	28	17
MAY	29	30	1	2	3	4	5	18
	6	7	8	9	10	11	12	19
	13	14	15	16	17	18	19	20
	20	21	22	23	24 Monthly Reports Due to DOE	25	26	21
JUNE	27	28	29	30	31	1	2	22
	3	4	5	6	7	8	9	23
	10	11	12	13	14	15	16	24
	17	18	19	20	21 Monthly Reports Due to DOE	22	23	25
	24	25	26	27	28	29	30	26

Trailblazer Activities

Trailblazer Activities